NUMERICAL SIMULATION OF NATURAL TURBULENT CONVECTION WITH VORTICITY VECTOR FORMULATION

BY

OTULO ONYANGO FILENTINUS

BEd.(Science)

I56/20471/2020

A research project submitted in Partial fulfillment of the requirement for the award of degree of Master of Science in Applied mathematics in the School of Pure and Apllied sciences of Kenyatta University.

MAY 2023

DECLARATION

This Project is my original work and has not been presented elsewhere for any other degree award.

Signature..... Date.....

OTULO ONYANGO FILENTINUS

I56/20471/2020

Declaration by supervisors.

This project has been submitted for examination with my approval as University Supervisor.

Dr. Kenndey Awuor

Kenyatta University

Department of Mathematics and Acturial Sciences

Signature..... Date.....

DEDICATION

I would like to dedicate this project to my My wife Maureen Anyango, my sons Luis and Jeremy and my daughter Ivana for their love and support.

ACKNOWLEDGMENT

My most heartfelt appreciation goes Teachers Service Commission's generous study leave policy that enabled me to pursue my master's degree from Kenyatta University, without their approval it would have been a tall order for me in this journey. The content of this document would not be complete without the technical, moral, and timely advice provided by my always motivating supervisor, Dr. Kennedy Awuor, and I would like to thank him for that. Thanks to all of my lecturers in the Mathematics Department at Kenyatta University, I was able to finish my degree under your guidance. Dr. Peter Mitili Dr. Peter Mitili (PhD) has been really helpful to me, and I appreciate all of his encouragement and advice during the result and discussion stage of this project. I'd also like to thank my wonderful wife, Maurine Anyango, for being there for me during my studies, the emotional support and peace of mind she offered unto me contributed a lot towards this great achievement. I give thanks to the Almighty God for all blessings and grace that he has showered upon me throughout my studies.

ABSTRACT

Turbulent natural convection in an enclosure plays a big part in heat transmission and the building environment. Sophisticated buildings around the world are outfitted with costly heaters and coolers to maintain comfortable temperatures for human existence, manufacturing, and sophisticated farming methods, a scenario that many people cannot afford. Over a time researchers have consistently developed a number of numerical study models to simulate the natural turbulent flow in these rectangular enclosures to solve complex problems associated with turbulent flows. In spite of several experimental studies and model simulations on the structure of natural turbulence convection, the fundamental mechanism in turbulent phenomena is still incomplete. Significant variations in experimental data and model simulation data in previous studies have been noted. This is because the unknown turbulent correlation coefficients resulting from the nonlinear terms of the turbulent flow control equations make it difficult to accurately determine fluid flow variables such as mean velocity distribution, temperature distribution and kinetic energy in a model simulation. Thus an accurate numerical prediction of natural turbulence convection is crucial to solving the nonlinear equations for subsequent practical applications. The performance of a numerical turbulence model k-ε in estimating the amount of heat transfer that occurs as a result of the naturally occurring turbulent convection that takes place within an air-filled rectangular enclosure is investigated in this work using vorticity vector formulation. The workflow of simulating the heat transfer which results from the action of natural convection within an enclosed rectangular cavity takes into account the effect of turbulence for the Rayleigh numbers $Ra = 1.552 \times 10^{10}$, $Ra = 9.934 \times 10^{11}$, $Ra = 1.552 \times 10^{13}$ and $Ra = 2.425 \times 10^{14}$. The Low-Reynolds-number turbulence k-ε model was employed in this numerical study to model the non linear relations $\overline{\nabla \cdot \rho u_i' u_j'}$ and $\frac{\partial C_p \overline{T' u_i'}}{\partial x_i}$ in the averaged Navier Stokes equation and energy equation respectively to complete the governing equations. Apart from the hot and cold walls, which are maintained at 308K and 288K, respectively, all of the walls of the enclosure are adiabatic. The vorticity vector formulation allowed the pressure term to be removed from the momentum equation. Finite difference approximations were used in the FLUENT program to solve the vorticity, energy, vector potential, and two resultant equations for each model together with their boundary conditions. The outcomes of the study for the distribution of the velocity and temperature components are presented, demonstrating that the number of contours and vortices increases proportionally with the Rayleigh Number. In addition, a higher Rayleigh number indicates more turbulence, which in turn implies a higher absolute value of the velocity hence increased Kinetic energy.

TABLE OF CONTENTS

List of Figures

NOMENCLATURE

ε	Energy Dissipation
ρ	Density
τ	Shear Stress
μ	Dynamic Viscousity
u,v,w	Velocity components in x,y,z direction
S_i	Body Forces
k	Turbulent kinetic energy
T	Thermodynamic Temperature
t	Time
g	Acceleration due to gravity
Re	Reynolds Number
Ra	Rayleigh Number
Pr	Prandtl Number
C_p	Specific heat capacity
P	Pressure forces
β	Thermal Expansion coefficient
ξ_i	Vorticity variables
α	Thermal diffusivity
U_t	Kinetic Turbulent Viscousity
σk and $\sigma\varepsilon$	Prandtl for turbulent kinetic energy

CHAPTER ONE

INTRODUCTION

1.1 Background of the Study

The fluid mechanics of today's world are intensely dominated by the chaotic and volatile motion known as turbulent flow. Even if the flow occurs naturally or is forced into the surrounding, heat, momentum, and mass exchange are caused by large-scale irregular vortex movements rather than diffusion. Many thermofluid devices such as pipes, boilers, compressors, integrated circuit motors, and capacitors are made to withstand the turbulence of the liquid flow around them. The movement of fluids is so closely related to these industrial disciplines of heat and mass transport that it is necessary to calculate turbulent flow before studying these fields.

The process through which heat and mass are transferred in fluids is known as convection, and it is closely related to the computation of heat exchange rates between liquid and solid borders. Laminar and turbulent flows are the two types of convective heat exchange in which the viscosity of the liquid is important. In turbulent flow, Small fluid components rotate in the flow direction and perpendicular to it, generating a turbulent mixture, while laminar flow is characterized by fluid elements traveling in parallel but not interacting with each other or the fluid in the adjacent paths.

There are two different kinds of convection, namely natural (free) convection and forced convection. In natural convection, fluid motion is caused solely by density differences derived from temperature gradients i.e. buoyancy driven and not by an external source. With the right surface geometry and orientation, a circular flow cycle of the liquid is created where the fluid around the heat source heats up and undergoes thermal expansion, becoming less dense and rising up while the cooler part of the fluid, which is more dense, sinks and displaces the warmer less dense fluid. This cycle only ends when the fluid is evenly heated throughout. If the movement of the fluid is caused by an external force such as stirring, or pumping then we have a forced convection. Also, it's critical to note that the fluid velocity and heat transfer coefficient that occur in natural turbulent flow are generally low compared to forced-controlled or man-controlled turbulent flow.

Only natural turbulent convection in rectangular enclosed cavities will be taken into account in this

project because it is an active area of research with numerous engineering applications including building insulation, nuclear reactor construction, electronic cooling devices, air conditioning systems, indoor air quality, and solar energy collectors among others. All these applications require a reliable data source for temperature and velocity distribution.

The turbulent convection motion in this project is considered to be bouyancy driven as a result of heating a fraction of one of the vertical walls and cooling an equal fraction of the opposite wall in the enclosure. Hence, maintaining a temperature difference between the two walls that are not adjacent while other walls of the enclosure are considered to be adiabatic.

1.1.1 Definitions

(i) Fluid

Any substance that flows relatively easily, often takes the shape of its vessel, and continuously deforms when subjected to even a minor shear stress.

(ii) Incompressible and compressible fluid.

A fluid is defined as being incompressible if its density remains constant under any flow; otherwise, the fluid is compressible.

(iii) Real and Ideal fluid.

The term "real fluid" refers to a substance that is viscous and capable of offering flow resistance while an ideal fluid is neither viscous nor resistant to flow.

(iv) Steady and Unsteady flow.

The fluid's velocity, pressure, and temperature distribution are constant in steady flow, but they fluctuate over time in unstable flow.

(v) Heat transfer

Involves making, using, converting, and exchanging thermal energy between different physical systems. Most energy transfer happens through conduction, convection, radiation, and phase changes.

(vi) Natural convection

As opposed to being caused by external forces, this form of flow is characterized by the fact that the motion of the fluid is produced internally, by density differences brought about by varying temperature gradients inside the fluid mass.

(vii) Turbulent flow

A liquid flow in which the microscopic components that make up the vortex travel in both along and across the direction of the flow causing the liquid to get mixed.

(viii) Rotational an Irrotational Flow

Rotational flow is characterized by fluid particles rotating while flowing along a streamline, while irrotational flow is not.

1.1.2 Assumptions

For the purpose of this study the following are some of the assumptions:-

(i) The enclosure has adaibatic walls.

(ii) The fluid under consideration is Newtonian.

(iii) The fluid is real and incompressible.

(iv) The fluid flow is determined by bouyancy.

1.2 Statement of the Problem

In spite of several experimental studies and model simulations on the structure of natural turbulence convection, the fundamental mechanism in turbulent phenomena is still incomplete. Significant variations in experimental data and model simulation data in previous studies have been noted, that is, the results obtained in the model studies were not entirely consistent with the experimental results. This is because the unknown turbulent correlation coefficients resulting from the nonlinear terms of the turbulent flow control equations make it difficult to accurately determine fluid flow variables such as mean velocity distribution, temperature distribution and kinetic energy in a model simulation. Thus an accurate numerical prediction of natural turbulence convection is crucial to solving the nonlinear equations for subsequent practical applications.

This study therefore, aims at developing a numerical model that will accurately simulate the natural turbulence convection in an enclosed cavity and that will help in accurately determining the velocity, temperature distribution and kinetic energy of the fluid in various enclosure components.

1.3 Objectives of the Study

1.3.1 General Objective

This study's overarching objective is to study natural turbulent flow in an enclosed rectangular cavity filled with air using vorticity vector formulation.

1.3.2 Specific Objectives

1. To numerically simulate the movement of fluid inside a closed system using the k-ε turbulent model.

2. To determine temperature dispersion in various enclosure regions

3. To determine the flow velocity in various areas of the enclosure.

4. To establish the kinetic energy changes in the enclosure as a function of Rayleigh number.

1.4 Significance of the Study

The research is limited to a computational domain for turbulent flow in an enclosed, rectangular, air-filled cavity. The research will focus on developing numerical models of natural turbulent convection in enclosed spaces, which are typically rectangular in shape. One vertical wall will be heated, while the other will be cooled. This study has various applications in engineering, manufacturing and farm fields. As a result, it will be beneficial for saving on computational tools and software that are needed to solve complex industrial problems involving turbulent flows, including, but not limited to, the heating of homes, cooling of electronic packages, refrigeration and storage of goods in the manufacturing industries. Furthermore, the findings of this study will also be helpful in determining optimal velocity and temperature fields hence allowing for the regulation of the microclimate through ventilation in homes, phytotherapeutic research facilities and manufacturing plants for efficient storage and preservation. The data obtained from this study will be useful in improving the accuracy of the previous model study data by significantly reducing the variations from the experimental studies. The research also aims at the determination of a better position to place the heater in an enclosure for effective heat energy distribution.

1.5 Justification of the Study

Numerous researchers have recently focused on the study of natural turbulence in an enclosed cavity, and significant progress has been made in this area, however, the significant variation in results from the model simulations to the experimental data is a gap that still exist. This research is being carried out in order to develop a model that will accurately solve the nonlinear terms of the turbulent flow in order to precisely simulate the turbulence and minimize the observed variations.

CHAPTER TWO

LITERATURE REVIEW

Numerous studies have been performed by different researchers on naturally occurring turbulence convection in enclosed cavities. In a rectangle-shaped confinement with partially insulated walls that transport heat at local substructure heating, Kuznetsov and Sheremet (2010) explored the effects of natural convection on turbulence. This is plausible given how heat is transferred in a frontier environment between convection and radioactivity. The mathematical formalism was based on the conventional k-ε turbulence equations with wall functions. The transient factor, thermal conductivity rate, and the Grashof number were all considered because of their unique impacts.

Sompong and Witayangkurn (2013) analyzed naturally occurring convection numerically in a trapezoidal enclosure with a wave-like top surface. In their work they studied the effects of wave amplitude, Rayleigh number and Darcy number on the free convection inside the cavity full of seawater of Prandtl number 7.2 by uniformly heating the bottom and partially heating the inclined boundaries. The results of their study demonstrate that different parameters affect convection motion, and that flow intensities and temperature distributions increase with increasing Rayleigh and Darcy numbers.The results also demonstrate that unlike Rayleigh numbers and Darcy numbers, the wave-like top surface has a negligible impact on the flow field pattern and temperature dispersion. Mayoyo et al. (2015) investigated heat transfer and free convective motion in a cylinder by studying the effects of increasing Reynolds, Froude, Euler, and Prandtl numbers on the temperature and velocity. According to the findings of their research, buoyancy forces caused by temperature differences between the top and bottom of cylinders influence significantly the air velocity within the enclosure, and that temperature and velocity are inversely related to cylindrical height.

Altaç and Uğurlubilek (2016) numerically evaluated models of free convection turbulence in two- and three-dimensional rectangular housing by solving 2D and 3D unsteady state of the governing equations of turbulent using FLUENT 6.3.26. Surface averaged mean Nusselt numbers were used to compare the obtained heat transfer rates for the 2D and 3D RANS models. According to their findings, 3D RANS model produces mean Nusselt numbers that are more accurate than 2D for larger Rayleigh numbers.

By creating isotherms and streamlines for various aspect ratios and making an observation on the

impact of the same parameter along hot and cold walls of an enclosure, Awuor and Gicheru (2017) statistically explored natural convection in rectangular enclosures. According to their study's findings, in horizontal housings heated from the side, the aspect ratio has a substantial influence on the temperature dispersion and fluid flow throughout the housing. It also causes a decrease in speed and leads the vortices to become more parallel, which reduces turbulence.

Karanja et al. (2017) mathematically analyzed naturally occurring turbulent convection at various aspect ratios and discovered that there is no uniformity to the distribution of velocity and temperature and that the aspect ratio of the enclosed cavity has a substantial impact on both their magnitudes and distributions.

In a large eddy simulation of free turbulent convection in an inclined tall cavity, Doukkali et al. (2018) employed the spectral method to SOLVE the Reyleigh-Benard problem.

Mutua (2019) conducted a numerical investigation of free turbulent convection inside a rectangular chamber that was heated and cooled in designated zones. Through their studies, they concluded that changing the Rayleigh number affects turbulence via changing the temperature distribution and the flow rate of the fluid.

Through experimental and model studies of heat and mass transfer at Reynolds numbers 40,000 and 80,000, Liu et al. (2021) investigated turbulence of internal cooling passages and the search for porous ribs that provide high thermal performance.

Using OpenFOAM, Loksupapaiboon and Suvanjumrat (2021) compared the predictions of two turbulence models for low turbulent convection in a rectangular enclosed chamber to the results found in the experimental literature. The results show that near the isothermal walls, temperature and velocity changed dramatically, and that natural convection caused by turbulence occurred in an air-filled square cavity.

Chaabane et al. (2021) Using a custom Fortran 90 program while utilizing the lattice Boltzmann technique as the foundation, studied the Rayleigh-Bénard Convection numerically. They left the right wall open and added two cozy circular and elliptical feathers to the lower wall. They used the Red-Boltzmann equation, which is connected to the Boussinesq method, to develop the nonlinear associated differential equations. The heat transfer rates from elliptical heat sources were greater than those from circular ones according to the findings of their Code verification, which also demonstrated good dependability of the existing mesoscopic numerical approach.

The foundation of the research by Talukdar and Tsubokura (2021), was the variation of cylinder position between eccentric and concentric positions along the enclosure's horizontal and vertical medians and diagonals. They conducted a mathematical study of free convection from a horizontally oriented cylinder at an eccentric position with a variation in aspect ratio of a cooled square cavity. To model the cylinder surface, they used quasi approximation conditions and the submerged boundary method. The heat transfer behavior with respect to Aspect ratio and Rayleigh number was determined using a

combo of thermal classificatory effects, enhanced convectional flow, and thermal effect between combustor periphery and enclosure wall. According to their findings, the circumferential location of the cylinder leads to a higher thermal exchange at an Aspect Ratio of 0.15 for Ra of 11140 and Aspect Ratio of 0.175 for Ra of 111400 for idiosyncratic position, and heat transfer was enhanced at the position closest to the vertical at Aspect Ratio greater than 0.175.

Natural turbulent convection modeling in a rectangle-shaped cavity was further carried out by Mugambi (2021), by using a k -ω SST turbulent model while considering the Boussinesq approximations and vector potential approximation to determine the best position of a heater and a cooler in enclosure. Her research's findings demonstrate that turbulence is reduced by rise in Rayleigh number, and that the location of heat source and the cooler has a significant impact on turbulence. As a result, the position of the heater and cooler affects how heat is distributed inside an enclosure. She also recommended placing the cooler and heater on the same side of the wall.

2.1 Research gaps

Researchers have conducted a number of studies on free convection in a rectangular duct and other enclosed cavities using different turbulence models and formulations to simulate and find out effects of turbulence parameters such as Rayleigh numbers, Prandtl numbers, Aspect ratios and Grashof numbers on the turbulent flow in enclosures. However, Application of vorticity vector formulation in k-ε turbulent model to simulate turbulent flow in three dimensional configuration, and to determine the fluid flow quantities as well as to find best location of the heat source in an enclosure with two vertical walls oppositely held as the heat and cooler source is an area that has not been researched on. Besides, results from experimental studies have significantly varied from the model simulation data. A course which will be addressed in this study.

CHAPTER THREE

METHODOLOGY

3.1 Introduction

Since the majority of industrial problems involving turbulent flows involve mass and heat transfers, it is crucial to take into account the dynamics of energy dissipation, multiple-point correlation, energy spectrum, and scalar transport. This is because explanations of turbulent flows ultimately rest in the physics of the momentum, energy, and vorticity fields as stated by Bernard and Wallace (2002)
In order to set the stage for discussion by creating fundamental equations that will clearly illustrate the physical processes that need to be investigated, understood, or predicted when solving natural turbulent convection, Natural turbulent convection will be studied in this chapter as a function of fluid flow characteristics in a rectangular enclosure with a fraction of one vertical wall heated and an equivalent percentage of the opposite wall cooled. Partial differential equations are used to describe these equations, and they express the conservation principles for mass, momentum, and energy.

3.2 General Governing Equations

Fluid dynamics is based on the three fundamental principles of mass, momentum, and energy conservation.

3.2.1 Continuity Equation

For a differential control volume, the mass conservation equation states that the net inflow rate over the controlled surface must be equal to the rate of mass increase within the controlled volume. Bansal (2005)
For the purposes of this study, a control volume with lengths dx, dy, dz in the directions of x, y, and z will be taken into consideration. considering that the inlet velocity components in the x, y, and z directions are u, v, and w, and that the density of the fluid element inside the control volume is denoted by rho.

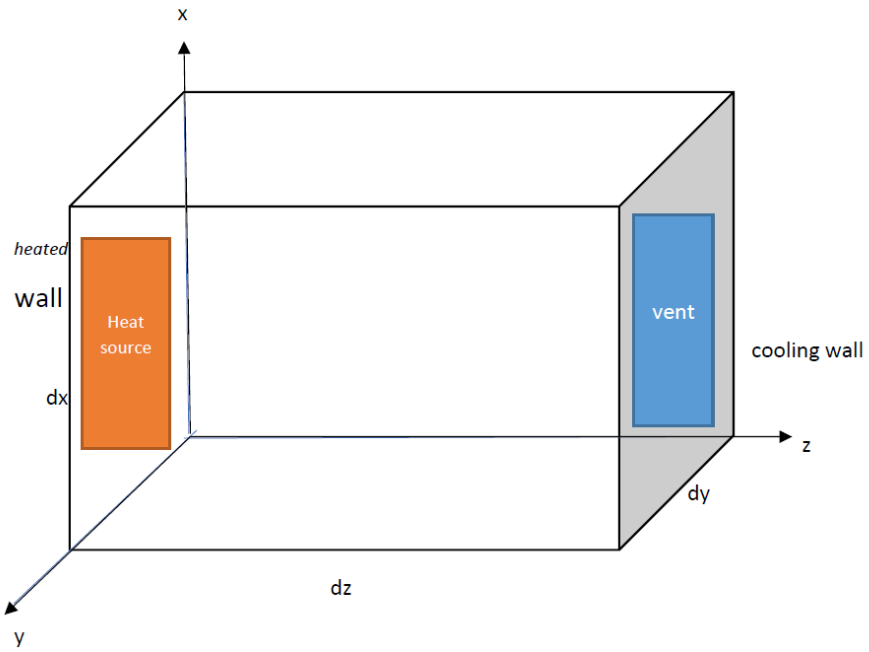

Figure 3.1: Control volume

In its simplest form, the equation of continuity in cartesian coordinates is shown as follows:

$$\frac{\partial \rho}{\partial t} + \frac{\partial}{\partial x}(\rho u) + \frac{\partial}{\partial y}(\rho v) + \frac{\partial}{\partial z}(\rho w) = 0 \tag{3.2.1}$$

But, $\frac{\partial \rho}{\partial t} = 0$ and hence equation $(3.2.1)$ becomes

$$\frac{\partial}{\partial x}(\rho u) + \frac{\partial}{\partial y}(\rho v) + \frac{\partial}{\partial z}(\rho w) = 0 \tag{3.2.2}$$

According to Currie(1974)The continuity equation may be summed up using cartesian tensor notation as

$$\frac{\partial \rho}{\partial t} + \frac{\partial}{\partial x_j}\left(\rho U_j\right) = 0 \tag{3.2.3}$$

This is given as in steady state

$$\frac{\partial}{\partial x_j}\left(\rho U_j\right) = 0 \tag{3.2.4}$$

3.2.2 Momentum Equation [Navier Stokes Equation]

The net force acting on a fluid mass is proportional to the rate of change in momentum per unit time, according to the rule of conservation of momentum, this forms the basis of this equation according to Schiestel (2010). According to Newton's second rule of the equation of motion, the force acting on a fluid of mass m is equal to the product of the fluid's mass m and the acceleration a it is experiencing. Assuming that m is always the same.

Since this is a relative vector, we may express it as a collection of three scalar relationships in terms of

the coordinate axes x, y, and z.

The momentum equations in x, y and z axes are as follows:-

$$\rho\left(u\frac{\partial u}{\partial x}+v\frac{\partial u}{\partial y}+w\frac{\partial u}{\partial z}+\frac{\partial u}{\partial t}\right)=-\frac{\partial p}{\partial x}+\mu\left(\frac{\partial^2 u}{\partial x^2}+\frac{\partial^2 u}{\partial y^2}+\frac{\partial^2 u}{\partial z^2}\right)+S_x \tag{3.2.5}$$

$$\rho\left(u\frac{\partial v}{\partial x}+v\frac{\partial v}{\partial y}+w\frac{\partial v}{\partial z}+\frac{\partial v}{\partial t}\right)=-\frac{\partial p}{\partial y}+\mu\left(\frac{\partial^2 v}{\partial x^2}+\frac{\partial^2 v}{\partial y^2}+\frac{\partial^2 v}{\partial z^2}\right)+S_y \tag{3.2.6}$$

$$\rho\left(u\frac{\partial w}{\partial x}+v\frac{\partial w}{\partial y}+w\frac{\partial w}{\partial z}+\frac{\partial w}{\partial t}\right)=-\frac{\partial p}{\partial y}+\mu\left(\frac{\partial^2 w}{\partial x^2}+\frac{\partial^2 w}{\partial y^2}+\frac{\partial^2 w}{\partial z^2}\right)+S_z \tag{3.2.7}$$

Where $S_x, S_y and S_z$ are body forces in x, y and z directions. $\frac{\partial p}{\partial x}, \frac{\partial p}{\partial y}, and \frac{\partial p}{\partial z}$ are pressure forces. The aforementioned equations are not in a conservative form because the fluid element is already moving together with the current. The general form of the momentum equation is

$$S_i+\frac{\partial}{\partial x_j}\left(\pi_{ij}\right)=\frac{\partial}{\partial t}\left(\rho u_i\right)+\frac{\partial}{\partial x_j}\left(\rho u_i u_j\right) \tag{3.2.8}$$

In the general equation (3.2.9), the terms πij and Si stand for the stress tensor and body forces per unit volume, respectively. The stress tensor for a Newtonian fluid as described by Currie:-

$$\pi_{ij}=-P\delta_{ij}+\tau_{ij} \tag{3.2.9}$$

Where τ_{ij} is the viscous stress tensor and δ_{ij} is the Kronecker delta with values of 1 for $i=j$ and 0 for $i\neq j$;

$$\tau_{ij}=\mu\left(\frac{\partial u_i}{\partial x_j}+\frac{\partial u_j}{\partial x_i}\right)+\mu_s\delta_{ij}\frac{\partial u_k}{\partial x_k} \tag{3.2.10}$$

Since the first coefficient of viscosity in this is mu and the second coefficient is μ_s, we may infer that the stress tensor is produced by

$$\pi_{ij}=-P\delta_{ij}+\mu\left(\frac{\partial u_i}{\partial x_j}+\frac{\partial u_j}{\partial x_i}\right)+\mu_s\delta_{ij}\frac{\partial u_k}{\partial x_k} \tag{3.2.11}$$

The general momentum equation for the Newtonian fluid we are concerned with in this study is obtained as below by writing Si as ρgi where gi represents gravitational force.

$$\rho g_i-\frac{\partial P}{\partial x_i}+\frac{\partial}{\partial x_j}\left[\mu\left(\frac{\partial u_i}{\partial x_j}+\frac{\partial u_j}{\partial x_i}\right)+\mu_s\delta_{ij}\frac{\partial u_k}{\partial x_k}\right]=\frac{\partial}{\partial t}\left(\rho u_i\right)+\frac{\partial}{\partial x_j}\left(\rho u_i u_j\right) \tag{3.2.12}$$

3.2.3 The Energy Equation

The law of conservation of energy serves as the foundation for the energy equation. The first rule of thermodynamics gives rise to the energy equation by stating that the rate of energy change in a fluid particle is equal to the rate of heat addition plus the rate of work performed on the particle, this according to Versteeg and Malalasekera (1995).

This can be described as

$$dQ = dE + dW \tag{3.2.13}$$

The energy equation as it was derived by Currie(1974) is as follows:

$$\frac{\partial}{\partial t}(C_p T) + \frac{\partial}{\partial x_j}(C_p u_j T) = \frac{\partial}{\partial x_j}\left(\lambda \frac{\partial T}{\partial x_j}\right) + \beta T\left(\frac{\partial p}{\partial t} + \frac{\partial u_j p}{\partial x_j}\right) + \phi \tag{3.2.14}$$

λ is thermal conductivity of the control volume

β is the volumetric coefficient of expansion

C_p is specific heat capacity at constant pressure. $\Phi = \tau_{ij}\frac{\partial U_i}{\partial x_j}$

k -Equation

$$\rho\frac{\partial k}{\partial t} + \rho\mu_j\frac{\partial k}{\partial x_j} = \frac{\partial}{\partial x_j}\left(\left(\mu + \frac{\mu_t}{\sigma k}\right)\frac{\partial k}{\partial x_j}\right) + \tau_{ij}\frac{\partial U_i}{\partial x_j} - \beta^*\rho k\varepsilon \tag{3.2.15}$$

ε - Equation

$$\rho\frac{\partial \varepsilon}{\partial t} + \rho\mu_j\frac{\partial \varepsilon}{\partial x_j} = \frac{\partial}{\partial x_j}\left(\left(\mu + \frac{\mu_t}{\sigma \varepsilon}\right)\frac{\partial \varepsilon}{\partial x_j}\right) + \alpha\frac{\varepsilon}{k}\tau_{ij} - \beta\rho\varepsilon^2 \tag{3.2.16}$$

3.3 Reynolds Decomposition and Statistical Averaging of Differential Equation.

Versteeg and Malalasekera (1995)states that turbulent flows happen when the Reynolds number (Re) exceeds the critical value $Re_{(}crt)$. Thus, the flow is described as being unpredictable, unstable, and chaotic. It is worthwhile to conclude that when the flow is turbulent, velocity and all other fluid flow parameters change in a random, unstable, and chaotic manner. A typical point velocity measurement, as illustrated below, demonstrates this unsteady, random, and chaotic nature.

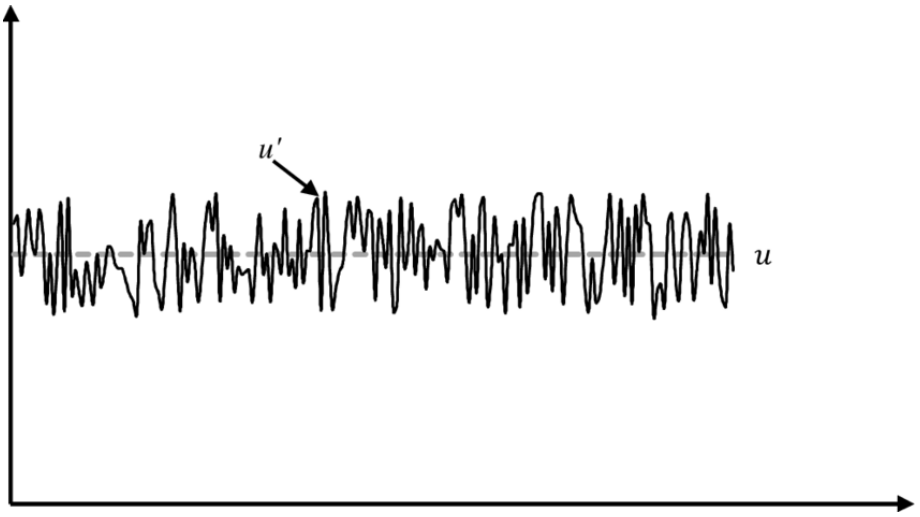

Figure 3.2: Changes in velocity over time at a given location in a turbulent flow

where U is the steady component and *U prime* U' is the fluctuation or perturbation component.
Since turbulence is time-dependent and has many different scales, it can be difficult to predict its behavior thus a mathematical technique known as Reynolds decomposition to disentangle a quantity's steady state from its random fluctuations is necessary. The velocity u in Figure 3.3 is decomposed using Reynolds Decomposition into a constant mean value $\bar{U}$ and a variable component U', as illustrated below:
$U = \bar{U} + U'$
The Navier Stokes Equations (3.2.4), (3.2.5), and (3.2.6) (3.2.7) must be decomposed in order to simplify them by substituting the velocity profile for the sum of the fluctuating and stable mean parts and averaging the results. The resulting equation has a nonlinear term, the Reynolds stress, which is used to describe the turbulence.
Thus, turbulent flow can be defined by the average values of flow variables (velocity U, pressure p, and so on) and some statistical aspects of their fluctuations (U', p' etc.)

3.3.1 Statistical averaging of differential equations

By proposing the concept of eddy viscousity, Joseph Valentin Boussinesq created the first mathematical treatment of a closure problem linked with turbulent flows in 1877. To conclude the system of equations, he hypothetically attributed the turbulence stresses to the mean flow, a theory that would subsequently be employed in calculating the Reynolds Stress. This approach was first employed in averaging the Narvier Stokes equation (Equation determining velocity and pressure) in turbulent flows in 1895, by splitting velocity and pressure quantities into mean and fluctuating portions this as stated bySchiestel (2010)
The Reynolds-averaged Navier-Stokes (RANS) equations, which regulate mean flow, are the result of averaging the governing equations. However, since the Navier-Stokes equations are nonlinear, the RANS equations continue to exhibit velocity fluctuations. As a result, we must obtain an equation con-

taining the mean velocity and pressure as a function of mean value flow by eliminating any fluctuating element of the velocity.

The Continuity Equation, the Navier-Stokes Equation, and the Energy Equation all have unsteady invariant that can be applied to solve turbulence problems. To model random fluctuations, statistical averaging of these equations is needed due to turbulence's time dependence and large length scales.

Turbulent flows may be described by the differential equations of momentum, mass and energy balances because these equations explain universal physical principles. Then, they can be solved, at least in principle. If all of the disturbances that have an effect on the flow can be represented analytically, then it should be possible to solve these equations in order to get flow parameters like the velocity and the pressure. These equations need to be solved using the time-averaged forms of their expressions since doing so will remove some of the fluctuation components.

$$u = \bar{u} + u' \tag{3.3.1}$$

$$v = \bar{v} + v' \tag{3.3.2}$$

$$p = \bar{p} + p' \tag{3.3.3}$$

$$\rho = \bar{\rho} + \rho' \tag{3.3.4}$$

$$T = \bar{T} + T' \tag{3.3.5}$$

Time Averaged Rules

$$\frac{1}{T}\int_0^T u dt = \bar{u} \text{ and } \frac{1}{T}\int_0^T \bar{u} dt = \bar{u'} = 0 \tag{3.3.6}$$

$$\frac{1}{T}\int_0^T v dt = \bar{v} \text{ and } \frac{1}{T}\int_0^T \bar{v} dt = \bar{v'} = 0 \tag{3.3.7}$$

$$\frac{1}{T}\int_0^T p dt = \bar{p} \text{ and } \frac{1}{T}\int_0^T \bar{p} dt = \bar{p'} = 0 \tag{3.3.8}$$

$$\frac{1}{T}\int_0^T \rho dt = \bar{\rho} \text{ and } \frac{1}{T}\int_0^T \bar{\rho} dt = \bar{\rho'} = 0 \tag{3.3.9}$$

t representing a significant portion of the time span.

When time averaging, the following additional criteria also apply.

1. $\bar{\bar{f}} = \bar{f}$
2. $\overline{f+g} = \bar{f} + \bar{g}$
3. $\frac{\overline{\partial f}}{\partial s} = \frac{\partial \bar{f}}{\partial x'}$
4. $\overline{\int f ds} = \int \bar{f} ds$
5. $\overline{f \cdot g} \neq \bar{f} \cdot \bar{g}$

3.3.2 Reynolds Decomposition

The exact solution of the governing equatons is required for full turbulent flow modeling. However, this is challenging since turbulent flows encompass multiple scales and the observed oscillations in turbulent flows are as a result of turbulent eddies but these oscillations do not make up the average flow. It is crucial in this case to devise a plan to reduce the level of complexity. The Reynolds-Averaged Navier-Stokes (RANS equations) are an approximation that allows us to classify the values of the variables that make up a flow into three groups: time-averaged values, mean values and fluctuating values.

Smoothing out fluctuations while yet allowing the overall trend to hold is the goal of the Reynolds decomposition. Using the Reynolds decomposition approach, the average value can be calculated by substituting a value for the sum of the constant and variable parts. Mean and fluctuating values are shown by the over bar and the prime values, respectively. As an example, we have defined the time-averaged variable $\bar{U}$ as follows with U taken as a fluid property.

$$\bar{U} = \frac{1}{T} \int_0^T U(x,t) dt \tag{3.3.10}$$

where

T is a long enough period of time for the quantity U to remain constant. Consequently, the quantity U can be represented as,

$$U = \bar{U} + U' \tag{3.3.11}$$

Time-averaging both sides yields (3.3.23).

$\bar{U} = \overline{\bar{U} + U'}$

It might be expressed simply as

$\bar{U} = \bar{U} + \bar{U}'$

Implying that

$$\bar{U}' = 0 \tag{3.3.12}$$

The value of the time average of the fluctuating component will eventually become zero.

Time Averaged Equation of Continuity

The most general version of the equation of continuity in cartesian co-ordinates is Equation 3.2.1. which is vectorially represented as:-

$$\frac{\partial \rho}{\partial t} + \nabla \cdot (\rho \vec{U}) = 0 \tag{3.3.13}$$

Substituting the velocity component U as $\bar{U} + U'$ and ρ as $\bar{\rho} + \rho'$ in equation (3.3.10) and taking the time average yields,

$$\overline{\frac{\partial (\bar{\rho} + \rho')}{\partial t}} + \nabla \cdot \left(\bar{\rho} + \rho'\right)\left(\bar{U} + U'\right) = 0 \tag{3.3.14}$$

which on expansion gives

$$\frac{\partial \left(\bar{\rho} + \overline{\rho'}\right)}{\partial t} + \nabla \cdot \left(\overline{\overline{\rho U}} + \overline{\bar{\rho} U'} + \overline{\rho' \bar{U}} + \overline{\rho' U'}\right) = 0 \tag{3.3.15}$$

Which can also be expressed as

$$\frac{\partial \bar{\rho}}{\partial t} + \frac{\partial \rho}{\partial t} + \frac{\partial}{\partial x_j}\left(\overline{\bar{\rho}\bar{U}_j}\right) + \frac{\partial}{\partial x_j}\left(\overline{\bar{\rho}\bar{U}_j}\right) + \frac{\partial}{\partial x_j}\left(\overline{\overline{U_j}\rho}\right) + \frac{\partial}{\partial x_j}\left(\overline{\rho' U'_j}\right) = 0 \tag{3.3.16}$$

Since $\overline{\bar{\rho} U'}$, $\overline{\rho' \bar{U}}$, and $\overline{\rho'}$ are equal to zero and $\overline{\overline{\rho U}} = \bar{\rho}\bar{U}$ the Time averaged equation of continuity becomes

$$\frac{\partial \bar{\rho}}{\partial t} + \frac{\partial}{\partial x_j}\left(\overline{\rho U_j}\right) + \frac{\partial}{\partial x_j}\left(\overline{\rho' U'_j}\right) = 0 \tag{3.3.17}$$

It is the continuity equation's Reynolds form.

Time Averaged Momentum Equation

Assuming that the Navier Stokes equation for a Newtonian fluid has the most generic form given by equation 3.2.12 and taking δ_{ij}= 1 and Substituting equations 3.3.1 and 3.3.3 in 3.2.7 we obtain:-

$$-\frac{\partial(\bar{P}+p')}{\partial x_i} + (\bar{\rho}+\rho')g_i + \frac{\partial}{\partial x_j}\left[\mu\left(\frac{\partial(\overline{u_i}+u_i)}{\partial x_j} + \frac{\partial\left(\overline{u_j}+u'_j\right)}{\partial x_i}\right) + \mu_s \frac{\partial(\overline{u_k}+u_k)}{\partial x_k}\right] = \frac{\partial(\bar{\rho}+\rho')(\overline{u_i}+u_i)}{\partial t} + \frac{\partial}{\partial x_j}(\bar{\rho}+\rho')\left(\bar{u}_i + u'_i\right)\left(\bar{u}_j +$$

Taking time averages on both sides we obtain

$$-\overline{\frac{\partial(\bar{P}+p')}{\partial x_l}} + \overline{(\bar{\rho}+\rho')g_i} + \overline{\frac{\partial}{\partial x_j}\left[\mu\left(\frac{\partial(\overline{u_i}+u_i)}{\partial x_j} + \frac{\partial\left(\overline{u_j}+u_j\right)}{\partial x_i}\right) + \mu_s \frac{\partial\left(\overline{u_k}+u'_k\right)}{\partial x_k}\right]} = \overline{\frac{\partial(\bar{\rho}+\rho')(\overline{u_i}+u_i)}{\partial t}} + \overline{\frac{\partial}{\partial x_j}(\bar{\rho}+\rho)\left(\bar{u}_i+u_i\right)\left(\bar{u}_j+u\right.}$$

With the following single averaging substituted and simplified

$$-\overline{\frac{\partial(\bar{P}+\bar{P})}{\partial x_i}} = -\frac{\partial}{\partial x_i}(\overline{\bar{P}+\bar{P}}) = -\frac{\partial}{\partial x_i}(\bar{P}+\bar{P}) = -\frac{\partial \bar{P}}{\partial x_i}$$

$$\overline{(\bar{\rho}+\rho')g_i} = (\overline{\bar{\rho}+\rho'})g_i = (\overline{\bar{\rho}}+\bar{\rho})g_i = \bar{\rho}g_i$$

$$\overline{\frac{\partial\left(\overline{u_i}+u'_i\right)}{\partial x_j}} = \frac{\partial}{\partial x_j}\left(\overline{\overline{u_i}+u'_i}\right) = \frac{\partial}{\partial x_j}\left(\overline{u_i}+\overline{u'_i}\right) = \frac{\partial}{\partial x_j}\overline{u_i}$$

$$\overline{\frac{\partial\left(\overline{u_j}+u'_j\right)}{\partial x_i}} = \frac{\partial}{\partial x_i}\left(\overline{\overline{u_j}+u'_j}\right) = \frac{\partial}{\partial x_i}\left(\overline{u_j}+\overline{u'_j}\right) = \frac{\partial}{\partial x_i}\overline{u_j}$$

$$\overline{\frac{\partial\left(\overline{u_k}+u'_k\right)}{\partial x_k}} = \frac{\partial}{\partial x_k}\left(\overline{\overline{u_k}+u'_k}\right) = \frac{\partial}{\partial x_k}\left(\overline{u_k}+\overline{u'_k}\right) = \frac{\partial}{\partial x_k}\overline{u_k}$$

$$\overline{\frac{\partial}{\partial t}\left(\bar{\rho}+\rho'\right)\left(\overline{u_i}+u'_i\right)} = \frac{\partial}{\partial t}\left(\overline{\rho u_i} + \overline{\rho u'_i} + \overline{\rho' u_i} + \overline{\rho' u'_i}\right) = \frac{\partial}{\partial t}\left(\overline{\rho u_i} + \overline{\rho' u'_i}\right)$$

$\frac{\partial}{\partial x_j}\left[\mu\left(\frac{\partial(\overline{u_i}+u_i)}{\partial x_j}+\frac{\partial(\overline{u_j}+u_j)}{\partial x_i}\right)+\mu_s\delta_{ij}\frac{\partial(\overline{u_k}+u_k)}{\partial x_k}\right]=\frac{\partial}{\partial x_j}\left[\mu\left(\frac{\partial\overline{u_i}}{\partial x_j}+\frac{\partial\overline{u_j}}{\partial x_i}\right)+\mu_s\delta_{ij}\frac{\partial\overline{u_k}}{\partial x_k}\right]$
The time averaged momentum equation in Reynolds form is obtained as

$$\frac{\partial}{\partial t}\left(\overline{\rho u_t}+\overline{\rho' u_t'}\right)+\frac{\partial}{\partial x_j}\left(\overline{\rho u_i u_j}+\overline{u_t\rho' u_j}\right)=-\frac{\partial\bar{p}}{\partial x_i}+\bar{\rho}g_i+\frac{\partial}{\partial x_j}\left(\overline{\tau_{ij}}-\overline{u_j\rho' u_i'}-\overline{\rho u_t' u_j'}-\overline{\rho' u_i' u_j'}\right) \tag{3.3.18}$$

and
$\overline{\tau_{ij}}=\mu\left(\frac{\overline{\partial u_i}}{\partial x_j}+\frac{\partial\overline{u_j}}{\partial x_i}\right)+\mu_s\delta_{iy}\frac{\partial\bar{u}_k}{\partial x_k}$

where REYNOLDS STRESS EQUATION is given by

$$\overline{\nabla\cdot\rho u_i' u_j'} \tag{3.3.19}$$

In cartesian coordinates the time averaged Navier Stokes equation becomes;

x - direction

$$\rho\left(\frac{\partial\bar{u}}{\partial t}+\bar{u}\frac{\partial\bar{u}}{\partial x}+\bar{v}\frac{\partial\bar{u}}{\partial y}+\bar{w}\frac{\partial\bar{u}}{\partial z}\right)=S_x-\frac{\partial\bar{\rho}}{\partial x}+\mu\left(\frac{\partial^2\bar{u}}{\partial x^2}+\frac{\partial^2\bar{u}}{\partial y^2}+\frac{\partial^2\bar{u}}{\partial z^2}\right)-\rho\left(\frac{\partial\overline{u'u'}}{\partial x}+\frac{\partial\overline{u'v'}}{\partial y}+\frac{\partial\overline{u'w'}}{\partial z}\right) \tag{3.3.20}$$

y-direction

$$\rho\left(\frac{\partial\bar{v}}{\partial t}+\bar{u}\frac{\partial\bar{v}}{\partial x}+\bar{v}\frac{\partial\bar{v}}{\partial y}+\bar{w}\frac{\partial\bar{v}}{\partial z}\right)=S_y-\frac{\partial\bar{\rho}}{\partial y}+\mu\left(\frac{\partial^2\bar{v}}{\partial x^2}+\frac{\partial^2\bar{v}}{\partial y^2}+\frac{\partial^2\bar{v}}{\partial z^2}\right)-\rho\left(\frac{\partial\overline{u'v'}}{\partial x}+\frac{\partial\overline{v'v'}}{\partial y}+\frac{\partial\overline{v'w'}}{\partial z}\right) \tag{3.3.21}$$

z-direction

$$\rho\left(\frac{\partial\bar{w}}{\partial t}+\bar{u}\frac{\partial\bar{w}}{\partial x}+\bar{v}\frac{\partial\bar{w}}{\partial y}+\bar{w}\frac{\partial\bar{w}}{\partial z}\right)=S_z-\frac{\partial\bar{\rho}}{\partial z}+\mu\left(\frac{\partial^2\bar{w}}{\partial x^2}+\frac{\partial^2\bar{w}}{\partial y^2}+\frac{\partial^2\bar{w}}{\partial z^2}\right)-\rho\left(\frac{\partial\overline{u'w'}}{\partial x}+\frac{\partial\overline{v'w'}}{\partial y}+\frac{\partial\overline{w'w'}}{\partial z}\right) \tag{3.3.22}$$

Time Averaged Energy Equation

Using the time averaging rules on the energy equation 3.2.9
$\frac{\partial}{\partial t}(C_pT)+\frac{\partial}{\partial x_j}\left(C_pu_jT\right)=\frac{\partial}{\partial x_j}\left(\lambda\frac{\partial T}{\partial x_j}\right)+\beta T\left(\frac{\partial p}{\partial t}+\frac{\partial u_jp}{\partial x_j}\right)+\Phi$
We obtain

$$\frac{\partial}{\partial t}\left(C_p\overline{\rho T}+C_p\overline{\rho' T'}\right)+\frac{\partial}{\partial x_j}\left(C_p\overline{\rho u_jT}\right)=\frac{\partial\bar{p}}{\partial t}+\frac{\partial\bar{p}}{\partial x_j}+\overline{u_{i'}\frac{\partial p'}{\partial x_j}}\quad+\frac{\partial}{\partial x_j}\left(\lambda\frac{\partial\bar{T}}{\partial x_j}-C_p\overline{\rho u_i'T'}-C_P\overline{\rho' u_iT'}\right)+\bar{\Phi} \tag{3.3.23}$$

$$\bar{\Phi}=\overline{\tau_{ij}}\frac{\partial\overline{u_i}}{\partial x_j}+\overline{\tau_{ij}'\frac{\partial u_i'}{\partial x_j}} \tag{3.3.24}$$

where $\frac{\partial C_p \overline{T'u_i'}}{\partial x_j}$ represent the thermal fluxes such as the parts of the temperature and velocity that fluctuate.

Turbulent flow Stress Tensor

The tensor form of equation 3.3.16 is as below.

$$\rho \frac{D\overline{u_l}}{Dt} = S_i - \frac{\partial \bar{p}}{\partial x_i} + \mu \Delta \bar{u}_\iota - \rho \left(\frac{\partial \overline{u_l u_J}}{\partial x_i} \right) \tag{3.3.25}$$

Where

$$\mu \Delta \bar{u}_i - \rho \left(\frac{\partial \overline{u_i u_j}}{\partial x_i} \right) = \mu \frac{\partial}{\partial x_j} \left(\frac{\partial u_i}{\partial x_j} \right) - \rho \frac{\partial}{\partial x_j} \overline{u_l u_j} = \frac{\partial}{\partial x_j} \left(\mu \frac{\partial u_i}{\partial x_j} - \overline{\rho u_i u_j} \right) \tag{3.3.26}$$

Total shear stress is denoted by the quantity included within the brackets in the preceding equation. It is stated as τ_{ij}

Hence, we may rewrite the previous equation, 3.3.16, as

$$\rho \frac{D\overline{u_l}}{Dt} = S_i - \frac{\partial \bar{p}}{\partial x_i} + \frac{\partial}{\partial x_j} \tau_{ij} \tag{3.3.27}$$

Considering the Eddy Viscosity principle approach, equation 3.3.27.above is called Reynods Averaged Navier Stokes equation (RANS).

and

$$\tau_{ij} = \mu \frac{\partial u_i}{\partial x_j} + \rho \left(v_t \left(\frac{\partial u_i}{\partial x_j} + \frac{\partial u_j}{\partial x_j} \right) - \frac{2}{3} k \delta_{ij} \right) \tag{3.3.28}$$

where the δ_{ij} is Kronecker delta function and v_t is turbulent viscosity.

According to Franke and Rodi (1993), In many turbulence models, Boussinesq's principle of eddy viscosity serves as the foundation.

$$-\overline{u_i' u_J'} = v_t \left(\frac{\partial u_i}{\partial x_j} + \frac{\partial u_j}{\partial x_i} \right) - \frac{2}{3} k \delta_{ij} \tag{3.3.29}$$

where k is the turbulence kinetic energy defined by

$$k = \frac{1}{2} \left(\overline{u^2} + \overline{v^2} + \overline{w^2} \right) \tag{3.3.30}$$

Consequently, the turbulence level determines the value of the turbulent vicosity v_t , which fluctuates with the flow of the liquid and the flow condition. The method of using a computer model of turbulent flow to determine the eddy viscosity v_t is called turbulence modeling.

3.4 k - ε model

A model of the second order, the k - ε Model, includes the turbulent kinetic energy K and the energy dissipation ε that are used to the calculation of v_t. In line with this, two additional equations will be solved in order to determine K and ε.

Energy dissipation ε is written as representation by means of dimensional analysis as shown and show its connection to characteristic length ℓ.

$$\varepsilon = C_D \frac{K^{2/3}}{\ell_m} \tag{3.4.1}$$

Where;

ℓ_m is the mixing length.

C_D is a coefficient of drag

K is a term of diffusion

ε is a term of dissipation.

Combining the equation of eddy viscosity with prandtl - Kolomogorov equation, the eddy viscosity equation becomes;

$$\mu_t = \rho C_\mu \frac{K^2}{\varepsilon} \tag{3.4.2}$$

Where C_μ = coefficient = 0.09 $\left(\mathrm{m}^2/\mathrm{s} \right)$

It is notable that the k-ε model accounts for the layered nature of the mixture and the turbulent viscosity by means of a buoyant term.

$$G = \frac{\mu_t}{\sigma_k} \cdot \frac{g}{\rho} \cdot \frac{\partial \rho}{\partial z} \tag{3.4.3}$$

Where;

$G > 0$ means unstable stratification

$G < 0$ means stable stratification

$G = 0$ means no stratification.

The following equations results from the k - ε Model.

Transport Equation for k

$$\frac{\partial}{\partial t}(\rho k) + \frac{\partial}{\partial x_i}(\rho k u_i) = \frac{\partial}{\partial x_j}\left[\left(\mu + \frac{\mu_t}{\sigma_k}\right)\frac{\partial k}{\partial x_j}\right] + G_K + G_b - \rho\varepsilon + F_k \tag{3.4.4}$$

Transport Equation for ε

$$\frac{\partial}{\partial t}(\rho \varepsilon) + \frac{\partial}{\partial x_i}(\rho \varepsilon u_i) = \frac{\partial}{\partial x_j}\left[\left(\mu + \frac{\mu_t}{\sigma_\varepsilon}\right)\frac{\partial \varepsilon}{\partial x_j}\right] + C_{1\varepsilon}\frac{\varepsilon}{K}(G_K + C_{3\varepsilon}G_b) - C_{2\varepsilon}\frac{\varepsilon^2}{k} + F_\varepsilon. \tag{3.4.5}$$

Where;

$G_k = -\rho\overline{u_l' u_j'}\frac{\partial u_j}{\partial x_i}$ represents the amount of kinetic energy produced by mean velocity gradients in turbulent flows. .

$G_b = \beta g_i \frac{\mu_t}{p_{rt}}\frac{\partial u_j}{\partial x_i}$ is the turbulent kinetic energy that is generated by buoyancy.

σ_k and σ_ε are Prandtl numbers for the kinetic energy of turbulent flow and the rate at which it is lost (dissipation).

γ_m stands for reaction coefficients

F_k and F_ε are user-created source terms.

The transport equation for k and energy dissipation equation ε on statistical averaging and Reynolds decomposition as derived by Tennekes et al. (1972) is as given below.

Time averaged equation for transport equation k

$$\frac{\partial}{\partial t}(\bar{\rho}k) + \frac{\partial}{\partial x_j}\left(\overline{\rho u_j k}\right) = \overline{u_j'\frac{\partial}{\partial x_j}\tau_{ij}} - \frac{1}{2}\frac{\partial}{\partial x_j}\left(\overline{\rho u_i' u_i' u_j'}\right) - \overline{\rho u_i' u_j'}\frac{\partial u_i}{\partial x_j} + \overline{\rho' u_i' g_i} - \overline{u_j'\frac{\partial p'}{\partial x_i}} \tag{3.4.6}$$

Time averaged equation for energy dissipation equation ε

$$\begin{aligned}\frac{\partial}{\partial t}\bar{\rho}\varepsilon + \frac{\partial}{\partial x_j}\overline{\rho u_j}\varepsilon = &-\frac{\partial}{\partial x_k}\left(\overline{\mu\mu_k'\frac{\partial u_i'}{\partial x_j}\frac{\partial u_i'}{\partial x_j}} + 2\nu\overline{\frac{\partial u_k'}{\partial x_i}\frac{\partial p'}{\partial x_i}}\right) - 2\mu\overline{\frac{\partial u_i'}{\partial x_k}\frac{\partial u_i'}{\partial x_j}\frac{\partial u_j'}{\partial x_j}} - 2\bar{\rho}\left(\overline{\nu\frac{\partial^2 u_i'}{\partial x_k \partial x_j}}\right)^2 + 2\nu\overline{\frac{\partial u_i'}{\partial x_j}\frac{\partial \rho'}{\partial x_j}}g_i \\ &-2\mu\frac{\partial \bar{u}_i}{\partial x_k}\left(\overline{\frac{\partial u_i'}{\partial x_i}\frac{\partial u_k'}{\partial x_j}} + \overline{\frac{\partial u_j'}{\partial x_i}\frac{\partial u_j'}{\partial x_k}}\right) - 2\mu\overline{\frac{\partial^2 u_i}{\partial x_j \partial x_k}}\overline{u_k'\frac{\partial u_i}{\partial x_j}}\end{aligned} \tag{3.4.7}$$

Model coefficients

The constants of the turbulence model are obtained from the experiments.The commonly used and updated values are from Launder and Sharma (1974) which are given as per the breakdown below.

$]C_{1\varepsilon}$	$C_{2\varepsilon}$	C_μ	σ_ε	σ_k
1.44	**1.92**	**0.09**	**1.3**	**1.0**

Figure 3.3: Constants of Turbulence model

3.5 Final Set of Equations

To make the above time averaged equation simpler, The over-bar in the preceding time-averaged equation for mean values of the variables throughout time will be replaced by upper case, while the prime denoting the fluctuating quantities will be written in lower case. Below are the complete set of equations for turbulent natural convection::-

$$\frac{\partial \rho}{\partial t} + \frac{\partial}{\partial x_j}\left(\rho U_j + \overline{\rho u_j}\right) = 0 \tag{3.5.1}$$

$$\frac{\partial}{\partial t}\left(\rho U_i + \overline{\rho u_i}\right) + \frac{\partial}{\partial x_j}\left(\rho U_i U_j + U_i \overline{\rho u_j}\right) = -\frac{\partial p}{\partial x_i} + \rho g_i + \frac{\partial}{\partial x_j}\left(\tau_{ij} - U_i \overline{\rho u_i} - \rho \overline{u_i u_j} - \overline{\rho u_i u_j}\right) \tag{3.5.2}$$

$$\frac{\partial}{\partial t}\left(C_p \rho T + C_p \overline{\rho T}\right) + \frac{\partial}{\partial x_j}\left(C_p U_j T\right) = \frac{\partial p}{\partial t} + U_j \frac{\partial p}{\partial x_j} + \overline{u_j \frac{\partial p}{\partial x_j}} + \quad \frac{\partial}{\partial x_j}\left(\lambda \frac{\partial T}{\partial x_j} - C_p \overline{U_t T} - C_p \overline{U_i T}\right) + \Phi \tag{3.5.3}$$

$$\frac{\partial}{\partial t}(\rho k) + \frac{\partial}{\partial x_j}\left(\rho U_j k\right) = \overline{u_j \frac{\partial}{\partial x_j} \mu \left(\frac{\partial u_i}{\partial x_j} + \frac{\partial u_j}{\partial x_l}\right)} - \frac{1}{2}\frac{\partial}{\partial x_j}\left(\overline{\rho u_i u_i u_j}\right) - \overline{\rho u_i u_j}\frac{\partial U_i}{\partial x_j} + \overline{\rho u_i} g_i - \overline{u_j \frac{\partial p}{\partial x_i}} \tag{3.5.4}$$

$$\begin{aligned} \frac{\partial}{\partial t}(\rho \varepsilon) + \frac{\partial}{\partial x_j}\left(\rho U_j \varepsilon\right) &= -\frac{\partial}{\partial x_k}\left(\overline{\mu \mu_k \frac{\partial u_i}{\partial x_j}\frac{\partial u_i}{\partial x_j}} + 2\nu \overline{\frac{\partial u_k}{\partial x_i}\frac{\partial p}{\partial x_i}} - \mu \frac{\partial \varepsilon}{\partial x_k}\right) \\ &+ 2\nu\left(\overline{\frac{\partial u_i}{\partial x_j}\frac{\partial \rho}{\partial x_j} g_i}\right) - 2\mu\left(\frac{\partial^2 u_i}{\partial x_i \partial x_k}\right)\mu \mu_k \left(\frac{\partial u_i}{\partial k_j}\right) - 2\mu \frac{\partial u_i}{\partial x_k}\left(\overline{\frac{\partial u_i}{\partial x_j}\frac{\partial u_k}{\partial x_j}} + \overline{\frac{\partial u_j}{\partial x_i}\frac{\partial u_j}{\partial x_k}}\right) \end{aligned} \tag{3.5.5}$$

3.6 Non - Dimensionalization

Non-Dimensionalisation is the adoption of suitable dimensionless scheme in the study of fluid dynamics, with the reason of reducing the number of parameters that are involved in the description of turbulent flow. Besides, it is also applicable in making the solutions bounded for instance temperature can be made dimensionless such that it varies from 0 to 1

In natural convection, the flow is not constrained by the boundaries, hence different flow regimes may experience different velocity scales. Reason being, the current isn't being propelled by the same set of variables. All physical attributes are often stated in non-dimensional forms by their corresponding values at a reference temperature, with the exception of the characteristic velocity, which is represented by an arbitrary velocity called U.

To achieve non-dimensionality, we use the following set of universal scaling variables, which are chosen because they are common to both the variables that result from statistical averaging and the variables that correspond to their fluctuation.

$X = \frac{x}{L_c}, Y = \frac{y}{L_c}, Z = \frac{z}{L_c}$

$U = \frac{u}{U_*}, V = \frac{v}{U_*}, W = \frac{w}{U_*}$, in vector form velocity components can be written as $\bar{U_{nj}} = \frac{\bar{U_j}}{U_*}$

$P = \frac{p-p_*}{\rho U_*^2}, t = \frac{t}{L_c/U_*}, \Theta = \frac{T-T_*}{\Delta T_*}$

$k_n = \frac{k}{{U_*}^2}, \varepsilon_n = \frac{\varepsilon}{{U_*}^3/L_c}, \mu_{t,n} = \frac{\mu_t}{\mu_c}, \alpha_{t,n} = \frac{\alpha_t}{\alpha_c}, \mu_n = \frac{\mu}{\mu_c}, \rho_n = \frac{\rho}{\rho_c}, C_{pn} = \frac{C_p}{C_{pc}}$

Where L_c denotes the described length, ΔT_* denotes the characterised temperature difference, and T_* denotes the suitable temperature that will result in Θ bounded in the solution area. Non-dimensional quantities include X, Y, Z, U, V, W, P, t, Θ, and all subscript n quantities, while the as subscript * represents a freely tunable variable signifying a dimensionality-free scheme.

Applying these non dimensional variables to the continuity equation 3.3.10 and using the statistical averaging rules, the equation is non dimensionalised as follows.

$\frac{\partial \rho}{\partial t} + \frac{\partial}{\partial x_j}\left(\rho U_j + \overline{\rho u_j}\right) = \frac{\partial \rho}{\partial t} + \frac{\partial\left(\rho U_j\right)}{\partial x_j} + \frac{\partial\left(\overline{\rho u_j}\right)}{\partial x_j} = 0$

$\frac{\partial \rho}{\partial t} = \frac{\partial \rho}{\partial \rho_n}\frac{\partial \rho_n}{\partial t_n}\frac{\partial t_n}{\partial t} = \frac{\rho_n U_*}{L_c}\frac{\partial \rho_n}{\partial t_n}$

$\frac{\partial U_j}{\partial x_j} = \frac{\partial U_j}{\partial U_{nj}}\frac{\partial U_{nj}}{\partial X_j}\frac{\partial X_j}{\partial x_j} = \frac{U_*}{L_c}\frac{\partial U_{nj}}{\partial X_j}$

$\rho\frac{\partial U_j}{\partial x_j} = \frac{U_*\rho_n\rho_c}{L_c}\frac{\partial U_{nj}}{\partial X_j}$

$\frac{\partial \rho}{\partial x_j} = \frac{\partial \rho}{\partial \rho_n}\frac{\partial \rho_n}{\partial X_j}\frac{\partial X_j}{\partial x_j} = \frac{\rho_c}{L_c}\frac{\partial \rho_n}{\partial X_j}$

$U_j\frac{\partial \rho}{\partial x_j} = \frac{\rho_c U_* U_{nj}}{L_c}\frac{\partial \rho_n}{\partial X_j}$

By chain rule, $\frac{\partial\left(\rho U_j\right)}{\partial x_j} = \rho\frac{\partial U_j}{\partial x_j} + U_j\frac{\partial \rho}{\partial x_j}$

Therefore,

$\frac{\partial\left(\rho U_j\right)}{\partial x_j} = \frac{U_*\rho_n\rho_c}{L_c}\frac{\partial U_{nj}}{\partial X_j} + \frac{\rho_c U_* U_{nj}}{L_c}\frac{\partial \rho_n}{\partial X_j}$

on simplification

$\frac{\partial\left(\rho U_j\right)}{\partial x_j} = \frac{U_*\rho_c}{L_c}\frac{\partial\left(\rho_n U_{nj}\right)}{\partial X_j}$

similarly, $\frac{\partial\left(\overline{\rho u_j}\right)}{\partial x_j} = \frac{U_*\rho_c}{L_c}\frac{\partial\left(\overline{\rho_n U_{nj}}\right)}{\partial X_j}$

summing all the non dimensional terms and simplifying the general form of continuity equation in non dimensional is as follows.

$\frac{\rho_n U_*}{L_c}\frac{\partial \rho_n}{\partial t_n} + \frac{U_* \rho_c}{L_c}\frac{\partial\left(\rho_n U_{nj}\right)}{\partial X_j} + \frac{U_* \rho_c}{L_c}\frac{\partial\left(\overline{\rho_n U_{nj}}\right)}{\partial X_j}$

$$\frac{\partial \rho_n}{\partial t_n} + \frac{\partial}{\partial X_j}\left(\rho_n U_{nj} + \overline{\rho_n U_j}\right) = 0 \tag{3.6.1}$$

Similarly, we apply the aforementioned approach to the mean momentum equation 3.3.16, averaged energy equation 3.3.21, kinetic energy transfer equation 3.4.4, and energy dissipation equation 3.4.5. The following are the resulting equations:-

$$\begin{aligned}\frac{\partial}{\partial t}\left(\rho_n U_{in} + \overline{\rho_n u_{ni}}\right) + \frac{\partial}{\partial x_{nj}}\left(\rho_n U_{nj} U_{nj} + U_{ni}\overline{\rho_n u_{nj}}\right) = -\left\{\frac{P_c}{\rho_c U_*^2}\right\}\frac{\partial P_n}{\partial x_{ni}} + \\ \left\{\frac{g L_c}{U_*^2}\right\}\rho g_{ni}\frac{\partial}{\partial x_j}\left(\left\{\frac{\mu_c}{\rho_c U_* L_c}\right\}\tau_{ij} - U_{nj}\overline{\rho_n u_{ni}} - \rho_n\overline{u_{ni}u_{nj}} - \overline{\rho_{nj}u_{ni}u_{nj}}\right)\end{aligned} \tag{3.6.2}$$

$$\begin{aligned}\frac{\partial}{\partial t_n}\left(C_{Pn}\rho_n\Theta + C_{Pn}\overline{\rho_n\theta}\right) + \frac{\partial}{\partial x_{nj}}\left(C_P\rho_n U_{nj}\Theta\right) = \left\{\frac{P_c}{C_{Pc}\rho_c\Delta T_*}\right\}\left[\frac{\partial P_n}{\partial t_n} + U_{nj}\frac{\partial P_n}{\partial x_{nj}} + \overline{u_{nj}}\frac{\partial P_n}{\partial x_j}\right] \\ + \frac{\partial}{\partial x_{nj}}\left(\left\{\frac{\lambda_c}{C_{Pc}\rho_c U_* L_c}\right\}\lambda\frac{\partial\Theta}{\partial x_{nj}} - C_P\rho_n\overline{u_i\theta} - C_P\overline{\rho_n u_{ni}\theta}\right) + \left\{\frac{\mu_c U_*}{C_{Pc}\rho_c\Delta T_* L_c}\right\}\Theta\end{aligned} \tag{3.6.3}$$

$$\begin{aligned}\frac{\partial}{\partial t_n}\rho_n k_n + \frac{\partial}{\partial x_j}\rho_n U_{nj} k_n = \left\{\frac{\mu_c}{\rho_c U_* L_c}\right\}\overline{u_{nj}\frac{\partial}{\partial x_{nj}}u_{nj}\left(\frac{\partial u_{ni}\partial x_{nj}}{+}\frac{\partial u_{nj}}{\partial x_{ni}}\right)} - \rho_n\overline{u_{ni}u_{nj}\frac{\partial U_{ni}}{\partial x_{nj}}} \\ -\frac{1}{2}\frac{\partial}{\partial x_j}\overline{P_n u_{ni}u_{nj}} + \left\{\frac{g L_c}{U^2 *}\right\}P_n U_{ni} - \left\{\frac{P_c}{P_c U^2}\right\}\overline{u_{nj}\frac{\partial P_n}{\partial x_{ni}}}\end{aligned} \tag{3.6.4}$$

$$\begin{aligned}\frac{\partial}{\partial t}p_n\varepsilon_n + \frac{\partial}{\partial x_{nj}}U_{nj}\varepsilon_n = -\left\{\frac{\mu_c}{P_c U_* L_c}\right\}\frac{\partial}{\partial x_{nk}}\left(\mu_n\mu_{nk}\frac{\partial u_{ni}}{\partial x_{nj}}\frac{\partial u_{nj}}{\partial x_{nj}} + 2\left\{\frac{P_c}{P_c U_*^2}\right\}\nu\overline{\frac{\partial u_{nk}}{\partial x_{ni}}}\frac{\partial P_n}{\partial x_{ni}} - m_n\frac{\partial\varepsilon_n}{\partial x_{nk}}\right) - \\ 2\left\{\frac{\mu_c}{P_{cU_* L_c}}\right\}\mu_n\frac{\partial u_{nj}}{\partial x_{nk}}\left(\frac{\partial u_{ni}}{\partial x_{nj}}\frac{\partial u_{nk}}{\partial x_{nj}} + \frac{\partial u_{ni}}{\partial x_{ni}}\frac{\partial u_{nj}}{\partial x_{nk}}\right) - 2\left\{\frac{\mu_c}{\rho_c U_* L_c}\right\}\mu_n\frac{\partial^2 u_i}{\partial x_{nj}\partial x_{nk}}\overline{u_{nk}\frac{\partial u_{ni}}{\partial x_{nj}}}\end{aligned} \tag{3.6.5}$$

Introducing a scheme for which the characteristic velocity is given as

$$U_* = \sqrt{g\beta\Delta T_* L_c} \tag{3.6.6}$$

the scheme above is focused on the momentum equation with an intention of of obtaining its scale factor. For the steady-state energy equation (3.54), it is necessary to ensure that the convection and conduction components are balanced, and therefore a technique is provided below to achieve this.

$$U_* = \frac{\lambda_c}{\rho_c C_p L_c} \tag{3.6.7}$$

On wards we shall consider all the variables and equations to be dimensionless and for the purpose of clarity, such that all the subscript n quantities indicating non dimensional variables, will be omitted.

Using the above schemes, the equations 3.5.1 to 3.5.5 will be respectively written in general form as:-

$$\frac{\partial \rho}{\partial t} + \frac{\partial}{\partial x_j}\left(\rho U_j + \overline{\rho U_j}\right) = 0 \tag{3.6.8}$$

$$\frac{\partial}{\partial t}\left(\rho U_i + \overline{\rho u_i}\right) + \frac{\partial}{\partial x_i}\left(\rho U_i U_j + U_i \overline{\rho u_J}\right) = -B_1 \frac{\partial p}{\partial x_i} + B_2 \rho g_i \frac{\partial}{\partial x_i}\left(B_3 \tau_{ij} - U_j \overline{\rho u_j} - \overline{\rho u_l u_J}\right) \tag{3.6.9}$$

$$\frac{\partial}{\partial t}\left(C_p \rho \Theta + C_p \overline{\rho \Theta}\right) + \frac{\partial}{\partial x_j}\left(C_p \rho U_j \Theta\right) = M_1 \left[\frac{\partial p}{\partial t} + U_j \frac{\partial p}{\partial x_j} + \overline{u_j \frac{\partial p}{\partial x_j}}\right] + \frac{\partial}{\partial x_j}\left(M_2 \lambda \frac{\partial \Theta}{\partial x_j} - C_p \rho \overline{u_l \Theta} - C_p \rho u_i \Theta\right) + M_3 \Phi \tag{3.6.10}$$

$$\frac{\partial}{\partial t}\rho k + \frac{\partial}{\partial x_j}\rho U_j k = T_1 \overline{u_j \frac{\partial}{\partial x_j} u_j \left(\frac{\partial u_j}{\partial x_j} + \frac{\partial u_j}{\partial x_j}\right)} - \frac{1}{2}\frac{\partial}{\partial x_j}\rho \overline{u_i u_j} \frac{\partial U_i}{\partial x_j} + T_2 \overline{\rho u_i} g_i - T_3 \overline{u_j \frac{\partial p}{\partial x_i}} \tag{3.6.11}$$

$$\begin{aligned} \frac{\partial}{\partial t}\rho \varepsilon + \frac{\partial}{\partial x_j}\rho U_j \varepsilon = & -\frac{\partial}{\partial x_k}\left(A_1 \mu u_k \frac{\partial u_i}{\partial x_j}\frac{\partial u_j}{\partial x_j} + 2A_2 V \overline{\frac{\partial u_k}{\partial x_i}\frac{\partial \rho}{\partial x_i}} - A_1 \mu \frac{\partial \varepsilon}{\partial x_k}\right) \\ & - 2A_1 \mu \frac{\partial U_i}{\partial x_j}\left(\overline{\frac{\partial u_i}{\partial x_j}\frac{\partial u_k}{\partial} + \frac{\partial u_j}{\partial x_j}\frac{\partial u_j}{\partial x_k}}\right) - 2A_1 \mu \frac{\partial^2 U_i}{\partial x_j \partial x_k} \overline{\mu u_k \frac{\partial u_i}{\partial x_j}} \end{aligned} \tag{3.6.12}$$

In which the coefficients B_1, B_2, B_3, M_1, M_2, M_3, T_1, T_2, T_3, A_1, A_2, A_3 and A_4 are represented in the table below.

		Scheme
U_*		$\sqrt{g\beta\Delta T L_c}$
B_1	$\frac{P_c}{\rho_c U_*^2}$	$\frac{EU.F_c}{\zeta\eta}$
B_2	$\frac{gL_c}{U_*^2}$	$\frac{1}{\zeta\eta}$
B_3	$\frac{\mu_R}{\rho_R U_* L_R}$	$\frac{1}{\sqrt{G_r}}$
M_1	$\frac{P_c}{C_{Pc}\rho_c\Delta T_*}$	$E_\mu E_C$
M_2	$\frac{\lambda_c}{C_{Pc}\rho_c U.L_c}$	$\frac{1}{P_r\sqrt{G_r}}$
M_3	$\frac{\mu_c U.}{C_{Pc}\rho_c\Delta T_* L_c}$	$E_c R_e{}^{-1}$
T_1	$\frac{\mu_c}{\rho_c U_* L_c}$	$\frac{1}{\sqrt{G_r}}$
T_2	$\frac{gL_c}{U_*{}^2}$	$\frac{i}{\zeta\eta}$
T_3	$\frac{P_c}{\rho_c U_*{}^2}$	$\frac{E_x F_r}{\zeta\eta}$
A_1	$\frac{\mu_c}{\rho_c U_* L_c}$	$\frac{1}{\sqrt{G_r}}$
A_2	$\frac{\mu_c P_c}{\rho_c{}^2 U.L_c}$	$\frac{E_a}{\sqrt{G_r}}$
A_3	$\left(\frac{\mu_c}{\rho_c U_* L_c}\right)^2$	$\frac{1}{\sqrt{G_r}}$
A_4	$\frac{g\mu_c}{\rho_c U_*{}^3}$	$\frac{Fr}{\sqrt{G_r}}$

Where

$$\frac{U_*}{gL_c} = Fr \text{ (Froude number)}; \quad \frac{\rho_R U_* L_c}{\mu_R} = \text{Re (Reynolds - number)}$$

$$\frac{P_c}{\rho_c U_*^2} = Eu \text{ (Euler number)}; \quad \frac{P_c}{\rho_c C_{PR} T_c} = Pn \text{ (Pressure number)}$$

$$(\mu_c g/\rho_c)/c_{pc}T_c = Gn \text{ (Gravity number)}; \quad \zeta = \frac{\Delta T_*}{T_c} \text{ (Non - dimensional temperature difference)}$$

$$\frac{\rho_c{}^2 C_{pc} g\beta\Delta T_* L_c}{\mu_c K_c} = \text{ Ra (Rayleigh - number)}; \quad \eta = \beta_R T_c$$

$$\frac{Ra}{\Pr} = Gr \text{ (Grashof number)}; \quad \frac{U^2{}_c}{C_{pc}\Delta T_*} = Ec \text{ (Eckert - number)}$$

$$\frac{\mu_c C_{pc}}{\lambda_c} = \text{ Pr (Prandtl number)}$$

In contrast to the equations already existing, the set of governing equations presented have more unknowns. More assumptions must be made in this area in order to lower the number of unknowns.

CHAPTER FOUR

TURBULENCE MODELING

4.1 Introduction

Mean flow equations describing turbulent transport of momentum, mass, and heat contain unknown turbulent correlations due to the statistical averaging of the general equations that regulate turbulent flows in rectangular enclosures as discussed in chapter three above.

These unknown turbulent correlations include $\overline{\nabla \cdot \rho u' u'}$ and $\frac{\partial C_p \overline{T' u'}}{\partial x_i}$ known as Reynolds stress equation and heat flux equation respectively. It is crucial to identify the essential connections and equations for determining these unknown turbulent correlations.

According to Awuor and Gicheru (2017), A turbulence model is precisely defined by the sets of relationships and equations used to calculate the unknown turbulent correlation coefficients arising from the statistical mean.

One of the earliest and most widely used approaches to modelling turbulent flows is the two-equation turbulence model. To account for phenomena like convection and turbulent energy diffusion that happen during turbulence, models use two more transport equations.

The kinetic energy k is the shared transport variable between the two turbulence models, while the second transported variable depends on the model employed. Common options include turbulent dissipation (ε) and specific dissipation (ω). The first variable, k, is regarded the basic equation and the most significant in turbulence modeling practice. Specifically, it characterizes the dynamics of turbulence's kinetic energy. Whereas the second is used to identify the time and/or velocity scales of the turbulence. This chapter explains how to model turbulence for a k-ε model with explicitly expressed boundary conditions.

4.2 Model Description

This research uses a velocity vector formulation to numerically simulate natural turbulent convection in three dimensions. The figure 4.1 below depicts the problem's geometry. The front face of the

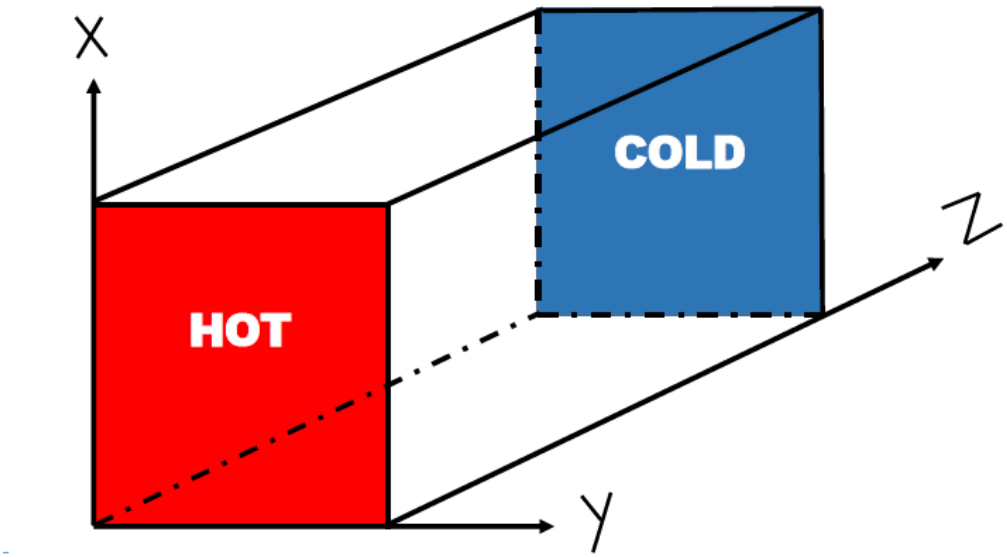

Figure 4.1: Model Geometry

rectangular enclosure, which is painted red, is heated, and the back face, which is painted blue, is cooled. Since Ampofo and Karayiannis (2003)'s experiment was conducted with high precision, their measurements were put in use. The enclosure's walls are 0.75m long, 0.75m high, and 1.5m wide which by calculation gives a Rayleigh number of 1.58×10^9 .

The cavity was maintained at 283K in a square cold wall face and 303K in a square hot portion. All four of the other walls are adiabatic. The rectangular cavity's boundaries are all hard, impermeable, and slip-free.

Further, the Boussinesq Approximation will be useful in this project as it will help in reduction of the governing equations.

4.3 Boussinesq Approximation

This method, which assumes that the density difference between hot and cold air in an enclosure is insignificant, is crucial for the analysis of buoyancy-driven flows in enclosures. Because the preceding requirements are valid for our current scenario, regardless of density being a function of temperature, we will use this approximation to transition to an even state.

4.3.1 Boussinesq Approximation Assumptions

1. Except for density, all fluid motion transport factors are assumed to be constant..

2. The density changes are insignificant.

3. The effects of viscous dissipation are insignificant..

4. The characteristics temperature difference is vanishingly small and essentially zero..

5. Due to buoyancy, there is a corresponding variation in density with temperature difference.

6. There is an internal heat source, and the fluid under examination is Newtonian.

4.3.2 Simplification of Governing Equations by Boussinesq Approximations.

If the above assumptions apply, buoyancy forces can be managed without the added complexity of fully compressible flow. Since, according to hypothesis five, The only thing that causes the density in the floating term to vary is the temperature, and even then, the change is barely noticeable, intuitively, this means that:-

$$\rho = \rho_c + (T - T_c)\left(\frac{\partial \rho}{\partial T}\right)_{T_c} \tag{4.3.1}$$

At constant pressure, the coefficient of thermal expansion can be calculated using the following formula:-

$$\beta_c = -\frac{1}{\rho_c}\left(\frac{\partial \rho}{\partial T}\right)_{T_c} \tag{4.3.2}$$

When we insert (4.4.2 into (4.4.1), we get

$$\rho = \rho_c\left(1 - \beta_c\left(T - T_c\right)\right) \tag{4.3.3}$$

Whose interpretation is known as Bousinessq approximation. The resultant equations that regulate natural convection in an enclosure are presented below after applying the Bousinessq approximation above and substituting them into the governing equations 3.5.8 to 3.5.12 in non-dimensional form; The equation for continuity, which is (3.5.8), is simplified as

$$\frac{\partial U_j}{\partial X_j} = 0 \tag{4.3.4}$$

The equation for the momentum (3.5.9) is:

$$\frac{\partial U_j}{\partial t} + \frac{\partial U_i U_j}{\partial x_j} = -\frac{B_1}{\rho_c}\frac{\partial P}{\partial x_i} - B_2 \Theta g_i + \frac{\partial}{\partial x_j}\left(B_3\left(\frac{\partial U_i}{\partial x_j} + \frac{\partial U_j}{\partial x_i}\right) - \overline{u_i u_j}\right) \tag{4.3.5}$$

Where $B_2 = (B_2)_{\text{old}}\ \beta_c \Delta T_*$ and the $(B_2)_{\text{old}}$ is shown in the table.

The energy equation (3.5.10) results into:

$$\frac{\partial \Theta}{\partial t} + \frac{\partial}{\partial x_j} U_j \Theta = \frac{\partial}{\partial x_j}\left(M_2 \frac{\partial \Theta}{\partial x_j} - \overline{u_j \theta}\right) \tag{4.3.6}$$

The turbulent kinetic k becomes:-

$$\frac{\partial k}{\partial t}+\frac{\partial}{\partial x_j}U_j k=T_1\overline{u_j\frac{\partial}{\partial x_j}v\left(\frac{\partial u_i}{\partial x_j}+\frac{\partial u_j}{\partial x_i}\right)}-\frac{\partial}{\partial x_j}\overline{u_j\left(\frac{u_i u_j}{2}+\frac{P}{\rho}\right)}+P_k+T_2G_k \tag{4.3.7}$$

Where $P_k=-\overline{u_i'u_j'}\frac{\partial u_j}{\partial x_i}$ and $G_k=\overline{\rho u_i}\frac{g_i}{\rho}$

The specific dissipation ε becomes

$$\frac{\partial \varepsilon}{\partial t}+\frac{\partial}{\partial x_j}U_j\varepsilon=-\frac{\partial}{\partial x_k}\left(A_1\overline{vu_k\frac{\partial u_i}{\partial x_j}\frac{\partial u_k}{\partial x_j}}+A_2v\overline{\frac{\partial u_k}{\partial x_i}\frac{\partial P}{\partial x_i}}-A_1v\frac{\partial \varepsilon}{\partial x_k}\right)-2A_1v\overline{\frac{\partial u_t}{\partial x_j}\frac{\partial u_i}{\partial x_j}\frac{\partial u_k}{\partial x_j}}-$$
$$2A_3\left(\overline{v\frac{\partial^2 u_i}{\partial x_k\partial x_j}}\right)^2+2A_4\frac{v}{\rho}\overline{\frac{\partial u_i}{\partial x_j}\frac{\partial P}{\partial x_i}}g_i-2A_1v\frac{\partial u_i}{\partial x_k}\left(\overline{\frac{\partial u_i}{\partial x_j}\frac{\partial u_k}{\partial x_j}}+\overline{\frac{\partial u_j}{\partial x_i}\frac{\partial u_j}{\partial x_k}}\right)-2A_1v\frac{\partial^2 u_i}{\partial x_j\partial x_k}\overline{U_k\frac{\partial u_i}{\partial x_j}} \tag{4.3.8}$$

Density is ignored everywhere except where it creates buoyancy forces in this situation. That is, the density from equation (4.3.7) cannot be ignored in the Gk since it causes buoyancy forces, which contribute to the formation of the notation, as argued by Awuor and Gicheru (2017) .

Stresses and heat flux in turbulent flows are calculated as below $\overline{u_i'u_j'}$ and $\overline{u_j\theta}$ in that order and are given as follows;

$$-\overline{u_i'u_J'}=v_t\left(\frac{\partial u_i}{\partial x_j}+\frac{\partial u_j}{\partial x_i}\right)-\frac{2}{3}k\delta_{ij} \tag{4.3.9}$$

And

$$\overline{u_j\theta}=-\frac{v_t}{\sigma T}\frac{\partial \Theta}{\partial x_j} \tag{4.3.10}$$

For which the v_t for k-ε model as seen earlier in chapter 3 is given by

$$v_t=c_\mu\frac{k^2}{\varepsilon} \tag{4.3.11}$$

4.4 Elimination of the pressure term from the Navier Stokes Equation

The momentum equation (4.3.5) makes use of the primitive variables pressure and velocity. The velocity and pressure variables in this equation must all be solved. Although the velocity-pressure formulation is capable of producing a solution, the pressure term makes it ineffective. This is because calculating velocities and pressures simultaneously using interpolation of equal orders is impossible. Therefore, in order to implement the most efficient numerical solutions, we will use the velocity-stream function technique in this project.

4.4.1 Vorticity stream function formulation

Dimensionless form of the continuity equation (4.3.4) and momentum equation (4.3.5) are extended and represented in two dimensions for a flow in a rectangular enclosure as follows:- Continuity equation

$$\frac{\partial U}{\partial X}+\frac{\partial V}{\partial Y}=0 \tag{4.4.1}$$

Momentum equation in x coordinates

$$\frac{\partial U}{\partial t}+U\frac{\partial U}{\partial x}+V\frac{\partial U}{\partial y}=-\frac{B_1}{\rho_c}\frac{\partial P}{\partial x}-B_2\theta\cos\gamma+\frac{\partial}{\partial x}\left((B_3+v_t)2\frac{\partial U}{\partial x}-\frac{2}{3}k\right)+\frac{\partial}{\partial y}\left((B_3+v_t)2\frac{\partial U}{\partial y}+\frac{\partial V}{\partial x}\right) \tag{4.4.2}$$

Momentum equation in y coordinates

$$\frac{\partial V}{\partial t}+U\frac{\partial V}{\partial x}+V\frac{\partial U}{\partial y}=-\frac{B_1}{\rho_c}\frac{\partial P}{\partial x}-B_2\Theta\sin\gamma+\frac{\partial}{\partial y}\left((B_3+v_t)\frac{\partial V}{\partial x}+\frac{\partial U}{\partial y}\right)+\frac{\partial}{\partial y}\left((B_3+v_t)2\frac{\partial V}{\partial y}-\frac{2}{3}k\right) \tag{4.4.3}$$

In this case, γ represents the angle between the gravitational vector and the x-axis. We introduce the stream function $\psi(x,y,t)$ to discover a solution to the continuity equation in two dimensions. The stream function's defining velocities are given as:-

$$U=\frac{\partial\psi}{\partial y} \tag{4.4.4}$$

$$V=-\frac{\partial\psi}{\partial x} \tag{4.4.5}$$

At some moment in time t_0, the stream function $\psi(x,y,t)$ may be written as $\psi(x,y,t0)$, and the previous equation is transformed into an exact or total differential along a vanishing streamline by treating the stream function as though it were $\psi(x,y,)$.

$$d\psi=\left(\frac{\partial\psi}{\partial x}\right)dx+\left(\frac{\partial\psi}{\partial y}\right)dy=0 \tag{4.4.6}$$

Based on this investigation, we conclude that, for a rectangular flow of an incompressible fluid, Along an instantaneous streamline, the stream function is continuous. The continuity equation(4.4.1) is thus obtained by differentiating equations (4.4.4) and (4.4.5) with regard to x and y, respectively. The streamlines may be seen and the number of simultaneous equations are reduced courtesy of the stream function. For instance, momentum equations in x and y coordinates (4.4.2) and (4.4.3) are merged together by introducing vorticity vector ξ.

Itatani et al. (2013), defined Vorticity vector as the curl $\vec{V}$ and $\vec{V}$ is the velocity vector, Vorticity vector

thus, is given by the equation below.

$$\vec{\xi} = \text{curl}\,\vec{V} = \nabla \times \vec{V} \tag{4.4.7}$$

By components, $\xi_x = \frac{\partial W}{\partial y} - \frac{\partial V}{\partial z}, \xi_y = -\left(\frac{\partial W}{\partial x} - \frac{\partial U}{\partial z}\right), \xi_z = \frac{\partial V}{\partial x} - \frac{\partial U}{\partial y}$, in three dimensions. For a flow in x-y dimension, $\xi_x = \xi_y = 0$ by application of right hand rule, thus $\xi_z = \frac{\partial V}{\partial x} - \frac{\partial U}{\partial y}$ defines the vorticity vector. Given in the form

$$\xi = \frac{\partial V}{\partial x} - \frac{\partial U}{\partial y} \tag{4.4.8}$$

When you substitute the resulting equations into equation (4.4.8) When you differentiate equation (4.4.4) with respect to x and equation (4.4.5) with respect to y, you will arrive at the following result:

$$\frac{\partial^2 \psi}{\partial x^2} + \frac{\partial^2 \psi}{\partial y^2} = -\xi \tag{4.4.9}$$

which explains the connection between stream function and vorticity.

The pressure factor is removed from the momentum equations by cross differentiating equations (4.4.2) and (4.4.3) with respect to y and x, respectively, and getting the difference between the resulting equations while considering the definition of vorticity equation (4.4.8). The parabolic vorticity transport equation is the resultant equation below:-

$$\frac{D\xi}{Dt} = (B_3 + v_t)\nabla^2 \xi + 2\left(\frac{\partial v_t}{\partial x}\frac{\partial \xi}{\partial x} + \frac{\partial v_t}{\partial y}\frac{\partial \xi}{\partial y}\right) - \left(\nabla^2 v_t\right)\xi + 2\left(\frac{\partial^2 v_t}{\partial x^2}\frac{\partial V}{\partial x} - \frac{\partial^2 v_t}{\partial y^2}\frac{\partial U}{\partial y} + 2\frac{\partial^2 v_t}{\partial x \partial y}\frac{\partial V}{\partial y}\right)$$
$$- B_2\left(\frac{\partial \Theta}{\partial x}\sin\gamma - \frac{\partial \Theta}{\partial y}\cos\gamma\right) \tag{4.4.10}$$

The equations (4.4.9) and (4.4.10) can substitute the continuity equation (4.4.1) and momentum equations (4.4.2) and (4.4.3) in primitive variable forms as long as It can be shown that the stream function and the vorticity boundary conditions are consistent with the velocity boundary conditions. The Neumann condition $\frac{\partial \psi}{\partial \eta} = 0$ is a condition that is incorporated into the boundary condition of the vorticity, as well as the Dirichlet condition ψ =constant, which have both been used previously.

A clear explanation of what wall vorticity means xi_a was done by Woods (1954), and the formula is given as;

$$\xi_a = \frac{3\psi_{a+1} - \psi_a}{(\Delta n)^2} - \frac{1}{2}\xi_{a+1} \tag{4.4.11}$$

Assuming that ξ changes linearly throughout this time interval, a+1 represents a location one mesh point from the border. Although the boundary conditions in such an indirect way of solving the Navier-Stokes equations are fairly difficult, the vorticity-stream formulation is preferred to the primitive variable version for a variety of reasons. . The following are some of the reasons for this preference:

1. There is an instantaneous solution to the continuity equation..

2. The use of a non-sequential finite difference grid is permitted.

3. The number of necessary differential equation solutions decreases.

4.4.2 Three-dimensional flow using a vector potential formulation

While the vorticity flow function formulation is only valid for two-dimensional flow issues, it can be used to approximate the flow function in three dimensions, where it does not exist. In contrast, a solenoidal vector field has a vector potential denoted by $\psi = \vec{\psi} = \vec{U}_i + \vec{V}_j + \vec{W}_k$. Because the equations to be solved increase rather than decrease, the analogy has not been used often. Furthermore, boundary conditions can be difficult to grasp.

Implementation in this regard was limited to the simplest scenarios in which the region is closed and connected. The continuity equation is satisfied immediately when the vector potential formulation is used, which is advantageous. Singh et al. (1993) considered the Rayleigh number in the range of 10^6 to10^7 and looked into a three-dimensional space where one of the vertical walls was heated and cooled by means of the flooring.

The vector potential ψ is defined as $U = \nabla \times \psi$. When it is presumed that this is a solenoid, then $\nabla.\psi = 0$. The stream function velocity components according to this formulation are:-

$$U = \frac{\partial \psi_3}{\partial y} - \frac{\partial \psi_2}{\partial z}, V = -\left(\frac{\partial \psi_3}{\partial x} - \frac{\partial \psi_1}{\partial z}\right), W = \frac{\partial \psi_2}{\partial x} - \frac{\partial \psi_1}{\partial y} \tag{4.4.12}$$

Based on the equation relating the stream function to the vorticity as,

$$\xi = -\nabla^2 \psi \tag{4.4.13}$$

As a result, we arrive at the three-dimensional vorticity equation as

$$\frac{\partial^2 \psi_1}{\partial x^2} + \frac{\partial^2 \psi_1}{\partial y^2} + \frac{\partial^2 \psi_1}{\partial z^2} = -\xi_1, \frac{\partial^2 \psi_2}{\partial x^2} + \frac{\partial^2 \psi_2}{\partial y^2} + \frac{\partial^2 \psi_2}{\partial z^2} = -\xi_2, \frac{\partial^2 \psi_3}{\partial x^2} + \frac{\partial^2 \psi_3}{\partial y^2} + \frac{\partial^2 \psi_3}{\partial z^2} = -\xi_3 \tag{4.4.14}$$

By rewriting the momentum equation as a vector potential of vorticity, we may be able to avoid the need for the pressure and primitive variables that we saw were contributing to the continuity equation's intractable nature. The vorticity vector ξ has three components:

$$\xi_1 = \frac{\partial W}{\partial y} - \frac{\partial V}{\partial z}, \xi_2 = -\left(\frac{\partial W}{\partial x} - \frac{\partial U}{\partial z}\right), \xi_3 = \frac{\partial V}{\partial x} - \frac{\partial U}{\partial y} \tag{4.4.15}$$

Ozoe et al. (1976) claims that the curl of the momentum equation (4.3.5) may be utilized to produce

the vorticity transport equation, thus the component form of the transport equation is as follows.

$$\begin{aligned}
&\frac{\partial \xi_1}{\partial t}+U\frac{\partial \xi_1}{\partial x}+V\frac{\partial \xi_1}{\partial y}+W\frac{\partial \xi_1}{\partial z}-\xi_1\frac{\partial U}{\partial x}-\xi_2\frac{\partial U}{\partial y}-\xi_3\frac{\partial U}{\partial z}\\
&=(B_3+v_t)\nabla^2\xi_1+\frac{\partial v_t}{\partial x}\frac{\partial \xi_1}{\partial x}+2\frac{\partial v_t}{\partial y}\frac{\partial \xi_1}{\partial y}+2\frac{\partial v_t}{\partial z}\frac{\partial \xi_1}{\partial z}-\frac{\partial v_t}{\partial y}\frac{\partial \xi_2}{\partial x}\\
&-\frac{\partial v_t}{\partial z}\frac{\partial \xi_3}{\partial x}-\left(\frac{\partial^2 v_t}{\partial y^2}+\frac{\partial^2 v_t}{\partial z^2}\right)\xi_1+\frac{\partial^2 v_t}{\partial x\partial y}\xi_2+\frac{\partial^2 v_t}{\partial x\partial z}\xi_3\\
&+2\left[\frac{\partial^2 v_t}{\partial x\partial y}\frac{\partial W}{\partial x}+\frac{\partial^2 v_t}{\partial y^2}\frac{\partial W}{\partial y}+\frac{\partial^2 v_t}{\partial y\partial z}\frac{\partial W}{\partial z}-\left(\frac{\partial^2 v_t}{\partial x\partial z}\frac{\partial V}{\partial x}+\frac{\partial^2 v_t}{\partial y\partial z}\frac{\partial V}{\partial y}+\frac{\partial^2 v_t}{\partial z^2}\frac{\partial V}{\partial z}\right)\right]
\end{aligned} \tag{4.4.16}$$

$$\begin{aligned}
&\frac{\partial \xi_2}{\partial t}+U\frac{\partial \xi_2}{\partial x}+V\frac{\partial \xi_2}{\partial y}+W\frac{\partial \xi_2}{\partial z}-\xi_1\frac{\partial V}{\partial x}-\xi_2\frac{\partial V}{\partial y}-\xi_3\frac{\partial V}{\partial z}=(B_3+v_t)\nabla^2\xi_2+2\frac{\partial v_t}{\partial x}\frac{\partial \xi_2}{\partial x}+\frac{\partial v_t}{\partial y}\frac{\partial \xi_2}{\partial y}+\\
&2\frac{\partial v_t}{\partial z}\frac{\partial \xi_2}{\partial z}-\frac{\partial v_t}{\partial x}\frac{\partial \xi_1}{\partial y}-\frac{\partial v_t}{\partial z}\frac{\partial \xi_3}{\partial y}-\left(\frac{\partial^2 v_t}{\partial x^2}+\frac{\partial^2 v_t}{\partial z^2}\right)\xi_2+\frac{\partial^2 v_t}{\partial x\partial y}\xi_1+\frac{\partial^2 v_t}{\partial y\partial z}\xi_3-B_3\frac{\partial \Theta}{\partial z}+2\left[\frac{\partial^2 v_t}{\partial x\partial z}\frac{\partial U}{\partial x}+\right.\\
&\left.\frac{\partial^2 v_t}{\partial y\partial z}\frac{\partial W}{\partial y}+\frac{\partial^2 v_t}{\partial z^2}\frac{\partial U}{\partial z}-\left(\frac{\partial^2 v_t}{\partial x^2}\frac{\partial W}{\partial x}+\frac{\partial^2 v_t}{\partial x\partial y}\frac{\partial W}{\partial y}+\frac{\partial^2 v_t}{\partial x\partial z}\frac{\partial W}{\partial z}\right)\right]
\end{aligned} \tag{4.4.17}$$

$$\begin{aligned}
&\frac{\partial \xi_3}{\partial t}+U\frac{\partial \xi_3}{\partial x}+V\frac{\partial \xi_3}{\partial y}+W\frac{\partial \xi_3}{\partial z}-\xi_1\frac{\partial W}{\partial x}-\xi_2\frac{\partial W}{\partial y}-\xi_3\frac{\partial W}{\partial z}=(B_3+v_t)\nabla^2\xi_3+2\frac{\partial v_t}{\partial x}\frac{\partial \xi_3}{\partial x}+2\frac{\partial v_t}{\partial y}\frac{\partial \xi_3}{\partial y}+\\
&\frac{\partial v_t}{\partial z}\frac{\partial \xi_3}{\partial z}-\frac{\partial v_t}{\partial x}\frac{\partial \xi_1}{\partial z}-\frac{\partial v_t}{\partial y}\frac{\partial \xi_2}{\partial z}-\left(\frac{\partial^2 v_t}{\partial x^2}+\frac{\partial^2 v_t}{\partial y^2}\right)\xi_3+\frac{\partial^2 v_t}{\partial x\partial z}\xi_1+\frac{\partial^2 v_t}{\partial y\partial z}\xi_2-B_2\frac{\partial \Theta}{\partial y}+2\left[\frac{\partial^2 v_t}{\partial x^2}\frac{\partial V}{\partial x}+\frac{\partial^2 v_t}{\partial x\partial y}\frac{\partial V}{\partial y}+\right.\\
&\left.\frac{\partial^2 v_t}{\partial x\partial z}\frac{\partial V}{\partial z}-\left(\frac{\partial^2 v_t}{\partial x\partial y}\frac{\partial U}{\partial x}+\frac{\partial^2 v_t}{\partial y^2}\frac{\partial U}{\partial y}+\frac{\partial^2 v_t}{\partial y\partial z}\frac{\partial U}{\partial z}\right)\right]
\end{aligned} \tag{4.4.18}$$

The vorticity transport equations (4.4.16), (4.4.17), and (4.4.18), as well as the vorticity equation (4.4.14), are used to replace the continuity and momentum equations given by equations (4.3.4) and (4.4.14). (4.3.5). The variables to be solved includes; ξ_1, ξ_2, ξ_3, U, V, W, Θ, k and ε. We can find out what the variables are by solving equations (4.4.16), (4.4.17), and (4.4.18) for ξ_1, ξ_2, and ξ_3 in turn, while U, V, and W are determined by solving equation (4.4.12), and k and ε are determined by making use of the equations for turbulent energy that Ince and Launde derived in 1989, which are as follows.;

$$\frac{\partial k}{\partial t}+\frac{\partial}{\partial x_j}U_j k=v_t\left(\frac{\partial U_i}{\partial x_j}+\frac{\partial U_j}{\partial x_i}\right)\frac{\partial U_i}{\partial x_j}-\varepsilon+\frac{\partial}{\partial x_j}\left[\left(T_2+\frac{v_t}{\sigma_k}\right)\frac{\partial k}{\partial x_j}\right]-T_2 g_i\overline{u_i\theta} \tag{4.4.19}$$

$$\begin{aligned}
&\frac{\partial \bar{\varepsilon}}{\partial t}+\frac{\partial}{\partial x_j}U_j\bar{\varepsilon}=C_{\varepsilon 1}\frac{\bar{\varepsilon}}{k}v_t\left(\frac{\partial U_i}{\partial x_j}+\frac{\partial U_j}{\partial x_i}\right)\frac{\partial U_i}{\partial x_j}-C_{\varepsilon 2}\frac{\bar{\varepsilon}^2}{k}+2F_1^2 v_t\left(\frac{\partial^2 U_j}{\partial x_j\partial x_k}\right)^2+\frac{\partial}{\partial x_j}\left[\left(F_1+\frac{v_t}{\sigma_\varepsilon}\right)\frac{\partial \bar{\varepsilon}}{\partial x_i}\right]+\\
&F_4 g_i\overline{U_i\theta}\frac{\bar{\varepsilon}}{k}+0.83\left(\frac{k^{\frac{3}{2}}}{\bar{\varepsilon}C_1 x_n}-1\right)^2\frac{\bar{\varepsilon}^2}{k}
\end{aligned} \tag{4.4.20}$$

for which the equation $\bar{\varepsilon}$ connects to the energy dissipation ε in the following manner.

$$\varepsilon = \bar{\varepsilon} + D \tag{4.4.21}$$

D is an abbreviation for the accelerated rate of deterioration outside of a solid barrier and close to a wall;

$$D = 2v\left(\frac{\partial k^{\frac{1}{2}}}{\partial x_j}\right)^2 \tag{4.4.22}$$

hence $\varepsilon = \bar{\varepsilon}$ because as one gets away from the solid boundary, D tends to zero. The constants of the turbulence k - ε model are given in the figure 3.4

4.5 Boundary Conditions

4.5.1 Velocity Boundary Conditions

Velocity is a unit used to indicate the conditions for fluid movement at a barrier. We utilize a no slip boundary condition, stating that a viscous fluid's velocity with regard to a solid boundary is zero. As the fluid travels, the molecules are thought to have a larger adhesive force than cohesive force. In a closed hollow, every barrier is impermeable and only travels in that direction. This means that the normal velocity component is 0 at all boundaries. An impermeable solid surface cannot permit mass to pass through it, hence, considering the X-Y plane, the surface velocity component is always zero since X = 0.

4.5.2 Temperature Boundary Conditions

The equation $\Theta = \frac{T-T_*}{\Delta T_*}$ provides the definition of the temperature in a non-dimensional form. The temperature difference between warm and cool surfaces, denoted by ΔT_*. That is $\Delta T_* = T_h - T_c$, where the selection of ΔT_* guarantees that it is constrained and ranges from 0 to 1. The following equations reflect the isothermal and adiabatic boundary conditions for heat flow, respectively.

$$\Delta T_* = Constant \tag{4.5.1}$$

$$\frac{\partial \Theta}{\partial n} = 0 \tag{4.5.2}$$

Where n indicates the wall's perpendicularity. The other four walls of the enclosure are kept in an adiabatic state since the core problem requires cooling on one wall and heating on the other. The Dirichlet boundary conditions are implemented as follows on the hot and cold walls. $\Theta_{hot} = 1$ and $\Theta_{cold} = 0$ while the Neumann boundary conditions are applied to the remaining four walls i.e $\frac{\partial \Theta}{\partial n} = 0$

4.5.3 Vector Potential Boundary Conditions

On the non-slip edge, the contour conditions are challenging. The tangential components on the surface and the normal derivatives of the normal component are the only ψ components that are not completely zero. For instance, considering the wall along the y-z level where $X = 0$ we have $\frac{\partial \psi_1}{\partial x}$, $\psi_2 = \psi_3 = 0$. In the same way, along the x-z level at Y=0 we have $\frac{\partial \psi_2}{\partial y}$, $\psi_1 = \psi_3 = 0$ and on x-y level at Z = 0, $\frac{\partial \psi_3}{\partial z}$, $\psi_1 = \psi_2 = 0$.

In our investigation, several Rayleigh numbers were used to produce the results, but the aspect ratios remained fixed at 2. The opposite cold wall is maintained at 288K, while the hot wall is maintained at 308K. While the other walls are kept adiabatic, the enclosure operates at a temperature of 298 K.

4.5.4 Vorticity Boundary conditions

Equation (4.4.13), produces the boundary conditions for vorticity. The equation's fundamental velocities can be used to express the elements of the no-slip vorticity (4.4.15). Taking into account the y-z boundary, where $\frac{\partial W}{\partial y} = \frac{\partial V}{\partial z} = \frac{\partial U}{\partial z} = \frac{\partial U}{\partial y} = 0$, by application of right hand rule, the vorticity boundary condition becomes $\xi_1 = 0, \xi_2 = -\frac{\partial w}{\partial x}, \xi_3 = \frac{\partial v}{\partial x}$.

Similarly, the wall along the x-y level where $\frac{\partial U}{\partial y} = \frac{\partial V}{\partial x} = \frac{\partial W}{\partial x} = \frac{\partial W}{\partial y} = 0$, giving vorticity boundary conditions of $\xi_1 = -\frac{\partial v}{\partial z}, \xi_2 = \frac{\partial U}{\partial z}, \xi_3 = 0$

For the wall along the x - z level, we have $\frac{\partial W}{\partial x} = \frac{\partial U}{\partial z} = \frac{\partial V}{\partial z} = \frac{\partial V}{\partial x} = 0$, resulting to $\xi_1 = \frac{\partial W}{\partial y}, \xi_2 = 0, \xi_3 = -\frac{\partial U}{\partial y}$.

The table below summarizes the aforementioned boundary criteria for vorticity and vector potential.

The equations (4.4.14), (4.4.15), (4.4.16), (4.4.17), (4.4.18), (4.4.19), and (4.4.20) provide a thorough mathematical model description for our $k - epsilon$ model along with these boundary conditions. The next chapter contains a review of these numerical techniques because the solutions to these equations cannot be found analytically, making the use of numerical methods appropriate for our investigation.

	X=0 $(y-z)$ plane	Y=0, $(x-z)$ plane	Z=0, $(x-y)$ plane
ψ_1	$\frac{\partial \psi_1}{\partial x}=0$	$\psi_1=0$	$\psi_1=0$
ψ_2	$\psi_2=0$	$\frac{\partial \psi_2}{\partial y}=0$	$\psi_2=0$
ψ_3	$\psi_3=0$	$\psi_3=0$	$\frac{\partial \psi_3}{\partial z}=0$
ξ_1	$\xi_1=0$	$\xi_1=\frac{\partial W}{\partial y}$	$\xi_1=-\frac{\partial V}{\partial z}$
ξ_2	$\xi_2=-\frac{\partial W}{\partial x}$	$\xi_2=0$	$\xi_2=\frac{\partial U}{\partial z}$
ξ_3	$\xi_3=\frac{\partial V}{\partial x}$	$\xi_3=-\frac{\partial U}{\partial y}$	$\xi_3=0$

Figure 4.2: Summary of vector potential and vorticity boundary conditions

CHAPTER FIVE

NUMERICAL METHODS

With the assistance of the finite difference approach, we are able to determine the solutions to the systems of nonlinear partial differential equations, coupled with their boundary conditions, that were obtained in the chapter that came before this one. To get an approximation of the partial differential equations in this scenario, we solve a set of linear equations that are based on the values of the functions at each mesh position. Due to the non-linear nature of these partial differential equations, an iterative method is required; the false transient method is an excellent choice for this particular application.
It is crucial to design an iteration procedure that takes the nonlinear nature of the equations into consideration.Kubíček et al. (1976) developed a method known as the false transient method, which adds false transient derivatives which is the process of transforming an equation into its parabolic equivalent. If a steady-state solution is sufficient, then the transient terms in the equations can be eliminated.

5.1 False Transient Method

In this strategy, transitory fictitious components $\frac{1}{\beta_\Theta}$ is added to the mean energy equation's time derivative, (4.3.6), $\frac{1}{\beta_\xi}$ is added to the vorticity transport equations,(4.4.16), (4.4.17), and (4.4.18), Both the turbulent kinetic energy equation (4.4.19) and the turbulent kinetic energy dissipation equation (4.4.20) are modified by the addition of $\frac{1}{\beta_k}$ and $\frac{1}{\beta\varepsilon}$, respectively. The coefficients β_Θ, β_ξ, β_k and β_ε are useful for establishing the right time step for the solution as well as enabling for speedier solution convergence. For estimating the differential equations, a mesh grid that works well must be chosen. In this way, the solution space is partitioned into rectangular volume elements, which, individually, stand in for volumes of depth one and are centred on respective mesh nodes, and whose coordinates are expressed in form of the integer variables i, j and k.

5.2 Finite Difference Approximations

The approach of approximation employing central, forward, and backward differences is utilized correctly; for example, we use backward and forward differences at corners and near edges. The con-

vective term is approximated using a hybrid differentiation technique that blends central and upwind patterns. In addition, non-uniform grids have been employed because convective terms are predominant. The spacing of the grid varies over the solution volume. Thus, parts with higher flow gradients use smaller spacing, while parts with lower flow gradients use larger distances.

5.2.1 Mesh Points

Natural turbulent convection flow in a structure is characterized by a thermally stratified center and a thin boundary layer around the walls. The border layer has very substantial flow gradients that call for large number of lattice points.In this case study, the enclosure's domain of the solution is divided into a network of uniform rectangular grids of 60 by 50 meshes with very fine spacing as shown below

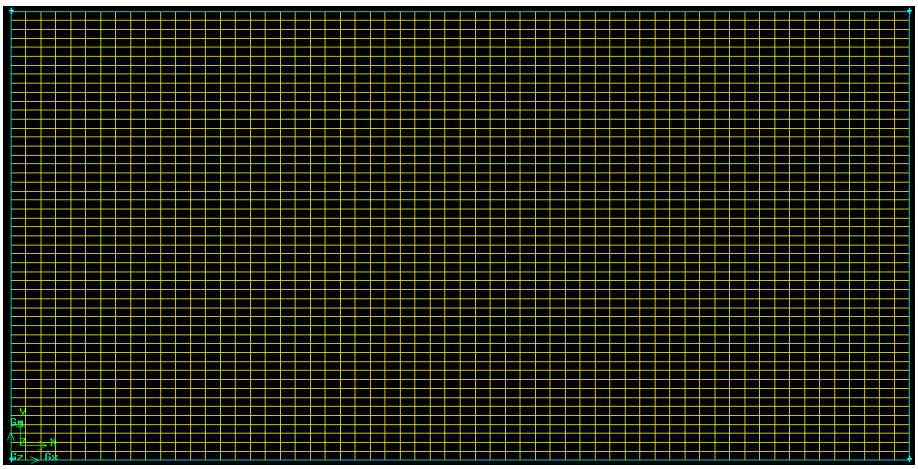

Figure 5.1: 60 by 50 mesh

Mesh points are represented as below,

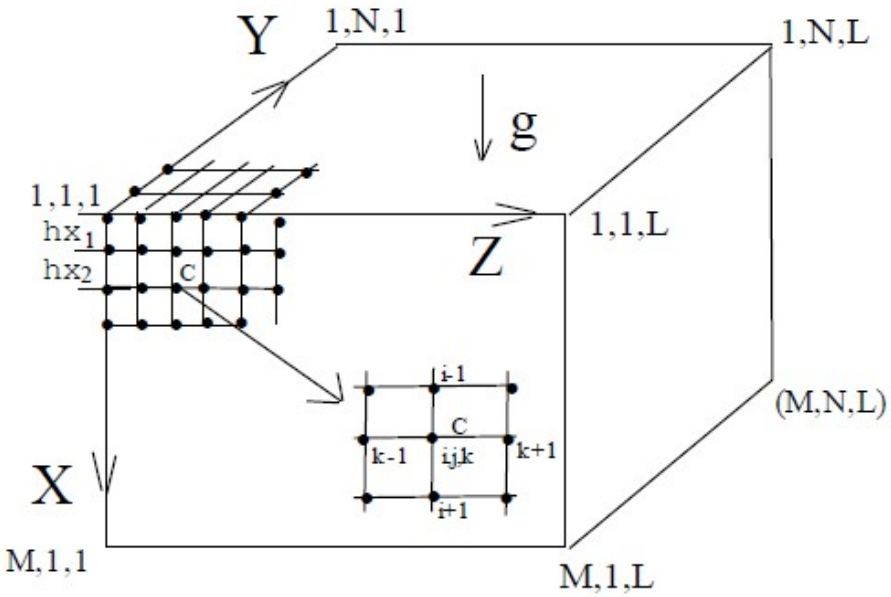

Figure 5.2: Mesh points

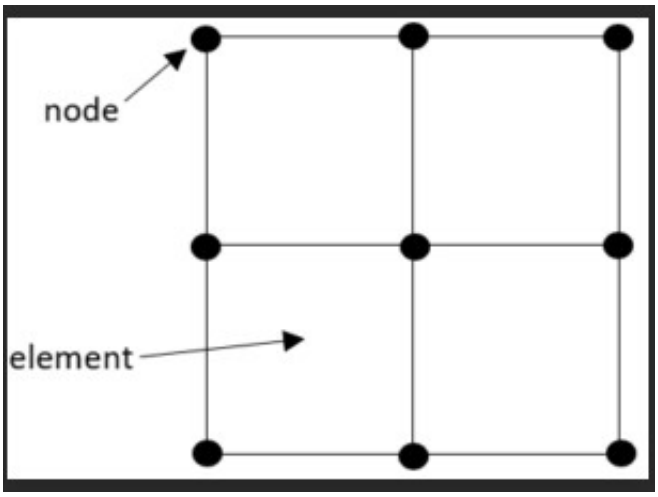

Figure 5.3: Nodes and elements

After utilising the finite difference approximation for PDEs, the following mesh point variables are recorded: $\emptyset = \emptyset(i,j,k)$

$$\emptyset(i-1) = \emptyset(i-1,j,k) \tag{5.2.1}$$

Differentials at mesh locations are given by,

$$\frac{\partial \emptyset}{\partial x} = \frac{h_i^2}{h_i^2 h_{i+1} + h_i h_{i+1}^2}\emptyset_{i+1} + \frac{-\left(h_i^2 + h_{i+1}^2\right)}{h_i^2 h_{i+1} + h_i h_{i+1}^2}\emptyset + \frac{-h_{i+1}^2}{h_i^2 h_{i+1} + h_i h_{i+1}^2}\emptyset_{i-1} \tag{5.2.2}$$

$$\frac{\partial \emptyset}{\partial y} = \frac{h_j^2}{h_j^2 h_{j+1} + h_j h_{j+1}^2}\emptyset_{j+1} + \frac{-\left(h_j^2 + h_{j+1}^2\right)}{h_j^2 h_{j+1} + h_j h_{j+1}^2}\emptyset + \frac{-h_{j+1}^2}{h_j^2 h_{j+1} + h_j h_{j+1}^2}\emptyset_{j-1} \tag{5.2.3}$$

$$\frac{\partial \emptyset}{\partial z} = \frac{h_k^2}{h_k^2 h_{k+1} + h_k h_{k+1}^2}\emptyset_{k+1} + \frac{-\left(h_k^2 + h_{k+1}^2\right)}{h_k^2 h_{k+1} + h_k h_{k+1}^2}\emptyset + \frac{-h_{k+1}^2}{h_k^2 h_{k+1} + h_k h_{k+1}^2}\emptyset_{k-1} \tag{5.2.4}$$

The second derivatives are given as below;

$$\frac{\partial^2 \emptyset}{\partial x^2} = \frac{2h_i}{h_i^2 h_{i+1} + h_i h_{i+1}^2}\emptyset_{i+1} + \frac{-2\left(h_i + h_{i+1}\right)}{h_i^2 h_{i+1} + h_i h_{i+1}^2}\emptyset + \frac{2h_{i+1}}{h_i^2 h_{i+1} + h_i h_{i+1}^2}\emptyset_{i-1} \tag{5.2.5}$$

$$\frac{\partial^2 \emptyset}{\partial y^2} = \frac{2h_j}{h_j^2 h_{j+1} + h_j h_{j+1}^2}\emptyset_{j+1} + \frac{-2\left(h_j + h_{j+1}\right)}{h_j^2 h_{j+1} + h_j h_{j+1}^2}\emptyset + \frac{2h_{j+1}}{h_j^2 h_{j+1} + h_j h_{j+1}^2}\emptyset_{j-1} \tag{5.2.6}$$

$$\frac{\partial^2 \emptyset}{\partial z^2} = \frac{2h_k}{h_k^2 h_{k+1} + h_k h_{k+1}^2}\emptyset_{k+1} + \frac{-2\left(h_k + h_{k+1}\right)}{h_k^2 h_{k+1} + h_k h_{k+1}^2}\emptyset + \frac{2h_{k+1}}{h_k^2 h_{k+1} + h_k h_{k+1}^2}\emptyset_{k-1} \tag{5.2.7}$$

We use the following designations to simplify the equations on the x-axis.

$D1_x = \frac{2h_i}{h_i^2 h_{i+1} + h_i h_{i+1}^2}$

$D2_x = \frac{-\left(h_i^2 + h_{i+1}^2\right)}{h_i^2 h_{i+1} + h_i h_{i+1}^2}$

$D3_x = \frac{-h_{i+1}^2}{h_i^2 h_{i+1} + h_i h_{i+1}^2}$

$D4_x = \frac{2h_i}{h_i^2 h_{i+1} + h_i h_{i+1}^2}$

$D5_x = \frac{-2(h_i+h_{i+1})}{h_i^2 h_{i+1}+h_i h_{i+1}^2}$
$D6_x = \frac{2h_{i+1}}{h_i^2 h_{i+1}+h_i h_{i+1}^2}$ The equations in the y- and z-axes are then simplified with the help of the corresponding indices.

Thus equation (5.2.2) and (5.2.5) reduces to, $\frac{\partial \emptyset}{\partial x} = D1_x \emptyset_{i+1} + D2_x \emptyset + D3_x \emptyset_{i-1}$ and $\frac{\partial^2 \emptyset}{\partial x^2} = D4_x \emptyset_{i+1} + D5_x \emptyset + D6_x \emptyset_{i-1}$ The application of these on equation (4.3.6), (4.4.12), (4.4.16) , (4.4.18), (4.4.19), (4.4.20) In order to derive the finite difference equations, the steps below are taken.

Mean equation energy equation (4.3.6) becomes:

$$\frac{\Theta^{n+1}-\Theta}{\beta_\Theta \Delta t} = -U\left(D1_x\Theta_{i-1} + D2_x\Theta + D3_x\Theta_{i+1}\right) - V\left(D1_y\Theta_{j-1} + D2_y\Theta + D3_y\Theta_{j+1}\right) - W\left(D1_z\Theta_{K-1} + D2_y\Theta + D3_z\Theta_{K+1}\right) + \left(M_2 + \frac{v_t}{\sigma_t}\right)\left(D4_x\Theta_{i-1} + D5_x\Theta + D6_x\Theta_{i+1} + D4_y\Theta_{j-1} + \left(D5_y\Theta + D6_y\Theta_{j+1} + D4_z\Theta_{k-1} + D5_z\Theta + D6_y\Theta_{k+1}\right) + \frac{1}{\sigma_T}\left[\left(D1_x v_{t_{i-1}} + D2_x v_t +\right).\right.\right.$$
$$\left.\left.\left(D3_x v_{t_{i+1}}\right)\left(D1_x\Theta_{i-1} + D2_x\Theta + D3_x\Theta_{i+1}\right) + \left(D1_y v_{t_{j-1}} + D2_y v_t + D3_y v_{t_{j+1}}\right)\left(D1_y\Theta_{j-1}+\right).\right.\right.$$
$$\left.\left.\left(D2_y\Theta + D3_y\Theta_{j+1}\right) + \left(D1_z v_{t_{k-1}} + D2_z v_t + D3_z v_{t_{k+1}}\right)\left(D1_z\Theta_{k-1} + D2_z\Theta + D3_z\Theta_{k+1}\right)\right] \tag{5.2.8}$$

Where $M_2 = \frac{1}{P_r\sqrt{G_r}}$.

Velocity equations resulting from (4.4.12) are as follows:-

$$U = D1_y\psi_{3j-1} + D2_y\psi_3 + D3_y\psi_{3j+1} - \left(D1_z\psi_{2k-1} + D2_z\psi_2 + D3_z\psi_{2k+1}\right) \tag{5.2.9}$$

$$V = D1_z\psi_{1k-1} + D2_z\psi_1 + D3_z\psi_{3k+1} - \left(D1_x\psi_{3i-1} + D2_x\psi_3 + D3_x\psi_{3i+1}\right) \tag{5.2.10}$$

$$W = D1_x\psi_{2i-1} + D2_x\psi_2 + D3_x\psi_{3i+1} - \left(D1_y\psi_{1j-1} + D2_y\psi_1 + D3_y\psi_{1j+1}\right) \tag{5.2.11}$$

Vector potential equations resulting from (4.4.14) are as follows:-

$$D4_x\psi_{1i-1} + D5_x\psi_1 + D6_x\psi_{1i+1} + D4_y\psi_{1j-1} + D5_y\psi_1 + D6_y\psi_{1j+1} + D4_z\psi_{1k-1} + D5_z\psi_1 + D6_z\psi_{1k+1} = -\xi_1 \tag{5.2.12}$$

$$D4_x\psi_{2i-1} + D5_x\psi_1 + D6_x\psi_{2i+1} + D4_y\psi_{2j-1} + D5_y\psi_2 + D6_y\psi_{2j+1} + D4_z\psi_{2k-1} + D5_z\psi_2 + D6_z\psi_{2k+1} = -\xi_2 \tag{5.2.13}$$

$$D4_x\psi_{3i-1} + D5_x\psi_3 + D6_x\psi_{3i+1} + D4_y\psi_{3j-1} + D5_y\psi_3 + D6_y\psi_{1j+1} + D4_z\psi_{3k-1} + D5_z\psi_3 + D6_z\psi_{3k+1} = -\xi_3 \tag{5.2.14}$$

$$\frac{\xi_1^{n+1}-\xi_1}{\beta_\xi \Delta t} = -U\left(D1_x\xi_{1i-1}+D2_x\xi_1+D3_x\xi_{1i+1}\right)-V\left(D1_y\xi_{1j-1}+D2_y\xi_1+D3_y\xi_{1j+1}\right)-$$
$$W\left(D1_z\xi_{1k-1}+D2_z\xi_1+D3_z\xi_{1k+1}\right)+\xi_1\left(D1_xU_{i-1}+D2_xU+D3_xU_{i+1}\right)+\xi_2\left(D1_yU_{j-1}+\right.$$
$$\left.D2_yU+D3_yU_{j+1}\right)+\xi_3\left(D1_zU_{k-1}+D2_zU+D3_zU_{k+1}\right)+\left(D3_xv_t\right)\left[D4_x\xi_{3i-1}+D5_x\xi_1+\right.$$
$$\left.D6_x\xi_{1i+1}+D4_y\xi_{1j-1}+D5_y\xi_1+D6_y\xi_{1j+1}+D4_z\xi_{1k-1}+D5_z\xi_1+D6_z\xi_{1k+1}\right]+$$
$$\left(D1_xv_{u-1}+D2_xv_t+D3_xv_{t+1}\right)\left(D1_x\xi_{1i-1}+D2_x\xi_1+D3_x\xi_{1t+1}\right)+2\left(D1_yv_{tj-1}+D2_yv_l+\right.$$
$$\left.D3_yv_{tj+1}\right)\left(D1_y\xi_{1j-1}+D2_y\xi_1+D3_y\xi_{1j+1}\right)+2\left(D1_zv_{tk-1}+D2_zv_t+\right.$$
$$\left.D3_zv_{tk+2}\right)\left(D1_z\xi_{1k-1}+D2_z\xi_1+D3_z\xi_{1k+1}\right)-\left(D1_yv_{tj-1}+D2_yv_t+D3_yv_{tj+1}\right)\left(D1_x\xi_{2i-1}+\right.$$
$$\left.D2_x\xi_2+D3_x\xi_{2t+1}\right)-\left(D1_zv_{tk-1}+D2_zv_t+D3_zv_{kk+1}\right)\left(D1_x\xi_{2i-1}+D2_x\xi_2+D3_x\xi_{2t+1}\right)-$$
$$\left(D4_yv_{tj-1}+D5_yv_t+D6_yv_{tj+1}+D4_zv_{tk-1}+D5_zv_l+D6_zv_{tk+1}\right)\xi_1+$$
$$\left[D1_y\left(D1_xv_{u-1,j-1}+D2_xv_{u,j-1}+D3_xv_{ui+1,j-1}\right)+D2_y\left(D1_xv_{ti-1}+D2_xv_ti+D3_xv_{ti+1}\right)+\right.$$
$$\left.D3_y\left(D1_xv_{ti-1,j+1}+D2_xv_{t,j+1}+D3_xv_{ti+1,j+1}\right)\right]\xi_2+\left[D1_z\left(D1_xv_{ti-1,k-1}+D2_xv_{t,k-1}+\right.\right.$$
$$\left.\left.D3_xv_{ti+1,k-1}\right)+D2_z\left(D1_xv_{ti-1}+D2_xv_t+D3_xv_{ti+1}\right)+D3_z\left(D1_xv_{ti-1,k+1}+D2_xv_{ti+1}+\right.\right.$$
$$\left.\left.D3_xv_{ti+1,k+1}\right)\right]\xi_3+2\left\{\left[D1_y\left(D1_xv_{ti-1,j-1}+D2_xv_{t,j-1}+D3_xv_{ti+1,j-1}\right)+\right.\right.$$
$$\left.\left.D2_y\left(D1_xv_{ti-1,j-1}+D2_xv_{t,j-1}+D3_xv_{ti+1,j-1}\right)\right]\left(D1_xW_{i-1}+D2_xW+D3_xW_{i+1}\right)+\right.$$
$$\left.\left(D4_yv_{tj-1}+D5_yv_t+D6_yv_{tj+1}\right)\left(D1_xW_{i-1}+D2_xW+D3_xW_{i+1}\right)+\left[D1_z\left(D1_yv_{tj-1k-1}+\right.\right.\right.$$
$$\left.\left.\left.D2_yv_{tk-1}+D3_yv_{tj+1k-1}\right)+D2_z\left(D1_yv_{tj-1}+D2_yv_l+D3_yv_{tj+1}\right)+D3_z\left(D1_yv_{t,j-1,k+1}+\right.\right.\right.$$
$$\left.\left.\left.D2_yv_{tk+1}+D3_yv_{tj+1k+1}\right)\right]\left(D1_xW_{i-1}+D2_xW+D3_xW_{i+1}\right)-\left[D1_z\left(D1_xv_{ti-1,k-1}+\right.\right.\right.$$
$$\left.\left.\left.D2_xv_{t,k-1}+D3_xv_{t+1,k-1}\right)+D2_z\left(D1_yv_{ti-1}+D2_yv_t+D3_yv_{ti+1}\right)+D3_z\left(D1_xv_{ti-1k+1}+\right.\right.\right.$$
$$\left.\left.\left.D2_xv_{tk+1}+D3_xv_{t,i+1,k+1}\right)\right]\left(D1_xV_{i-1}+D2_xV+D3_xV_{i+1}\right)+\left[D1_z\left(D1_yv_{tj-1,k-1}+\right.\right.\right.$$
$$\left.\left.\left.D2_yv_{tk-1}+D3_yv_{tj+1k-1}\right)+D2_z\left(D1_yv_{tj-1}+D2_yv_t+D3_yv_{t,j+1}\right)+AZ3\left(D1_yv_{tj-1,k+1}+\right.\right.\right.$$
$$\left.\left.\left.D2_yv_{tk+1}+D3_yv_{tj+1k+1}\right)\left(D1_yV_{j-1}+D2_yV+D3_yV_{j+1}\right)\left(D4_yV_{tk-1}+D5_yV_t+\right.\right.\right.$$
$$\left.\left.\left.D6_yV_{tk+1}\right)\left(D1_yV_{k-1}+D2_yV+D3_yV_{k+1}\right)\right]\right\} \tag{5.2.15}$$

5.2.2 Turbulent flow essential input

The input of turbulent flow presented in the following table is necessary to simulate and acquire the results of the project as indicated in the subsequent chapter.

Input	Value	
Geometry		Aspect Ratio
Ra =1.552 x 10^{10}	2 x 1 x 1	2
Ra =9.934 x 10^{11}	8 x 4 x 4	2
Ra =1.552 x 10^{13}	20 x 10 x 10	2
Ra =2.425 x 10^{14}	50 x 25 x 25	2
Models		
Energy	On	
Viscous	Standard $k-\varepsilon$	
Material Properties at 298 K		
Density	1.1845kg/m^3	
Dynamic Viscousity	1.8444E-05 Kg/ms	
Specific heat capacity	1.0063E+03 J/Kg/K	
Thermal Conductivity	0.025969 W/m.K	
Thermal Expansion coefficient	3.3540E-03 1/K	
Prandtl number	0.7147	
Gravitational force	9.81 m/s^2	
Solution models		
Pressure	PRESTO	
Momentum	First Order Upwind	
Turbulent Kinetic Energy	First Order Upwind	
Turbulent Dissipation Rate	First Order Upwind	

Figure 5.4: Turbulent flow important input

CHAPTER SIX

RESULTS AND DISCUSSION

6.1 Distribution of streamlines

A streamline is the path traced by a massless particle moving with the flow. Resistance to flow in fluids like air is minimised along these lines, which extend at right angles to the flow direction. For this study, the results were found for Rayleigh numbers between 1.522×10^{10} and 2.452×10^{14}. The figures show how the streamlines are spread out, and they prove that two separate vortices are in motion. A vortex is defined as a swirling fluid motion. It has been noticed that as the Rayleigh number increases, so does the velocity, with the minimum being 1.30×10^{-1}Kg/s and maximum being 2.53×10^{1}Kg/s. The movement of the streamlines originates from the hot wall. Thus, this conclusion is consistent with the idea of heat transfer. The buoyancy forces, the magnitude of the vortices, and the strength of the stream function all rise with the Rayleigh number. The results reported here agree with those from the experimental studies published DOĞAN and DOĞAN (2017).

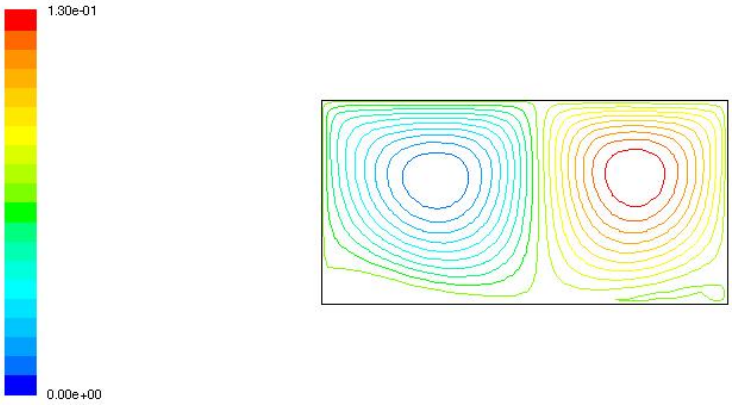

Figure 6.1: $Ra = 1.552 \times 10^{10}$

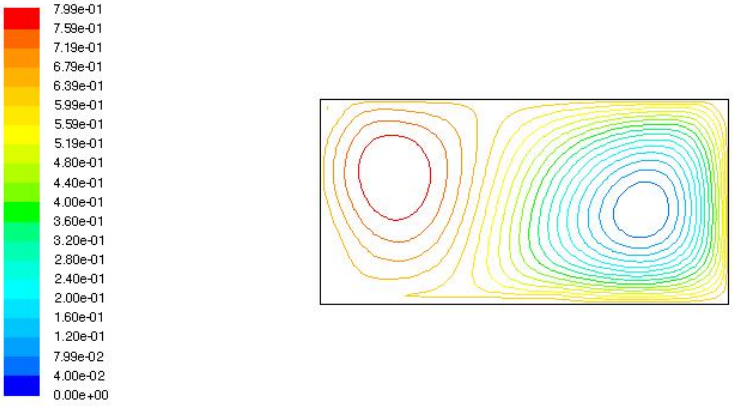

Figure 6.2: $Ra = 9.934 \times 11^{10}$

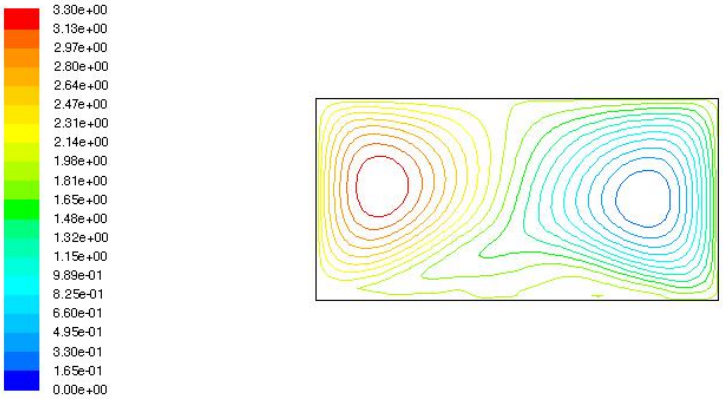

Figure 6.3: $Ra = 1.552 \times 10^{13}$

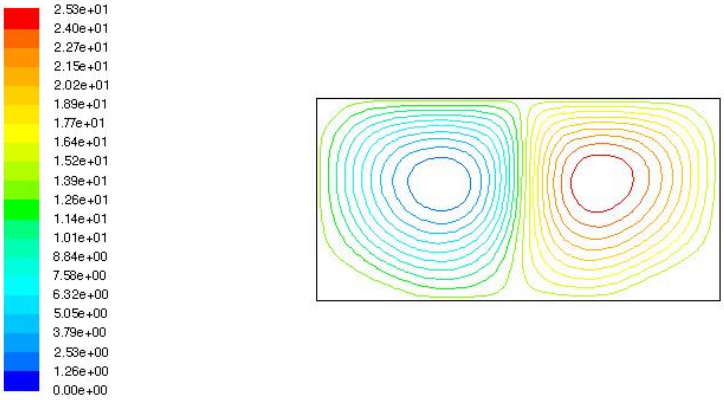

Figure 6.4: $Ra = 2.425 \times 10^{14}$

6.2 Contours of Velocity magnitudes (m/s)

The figures below 6.1, 6.2, 6.3, 6.4 represents the contours of velocity magnitude. As the number of Rayleighs grows, there is a corresponding increase in the number of vortices. Furthermore, the streamlines on the heated wall grow as the number of Rayleigh rises. The flow becomes more chaotic with rising Rayleigh number, leading to a rise in velocity magnitude, as shown in figures 6.1 and 6.4, where a slowest velocity of 0.308 m/s was recorded and the maximum velocity was measured at 2.23 m/s, respectively. These findings are consistent with those of the practical investigational study by DOĞAN and DOĞAN (2017), which found that a higher Rayleigh number leads to a greater velocity.

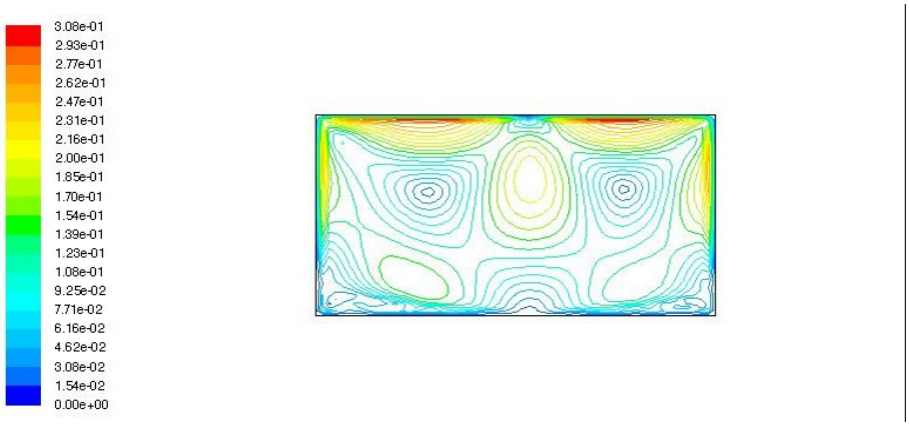

Figure 6.5: $Ra = 1.552 \times 10^{10}$

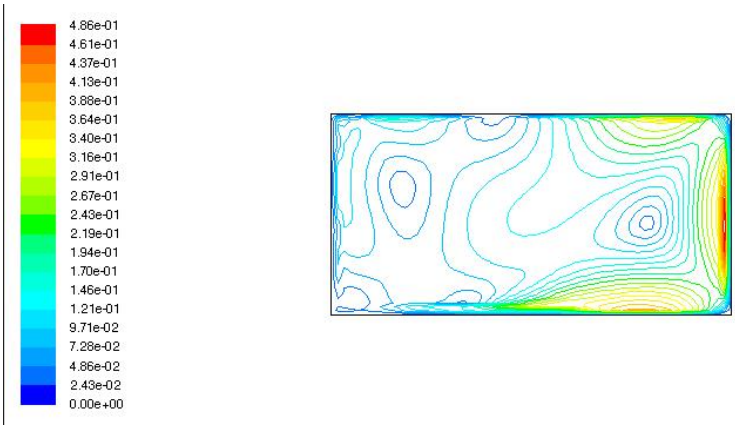

Figure 6.6: $Ra = 9.934 \times 10^{11}$

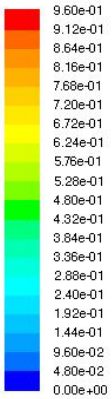

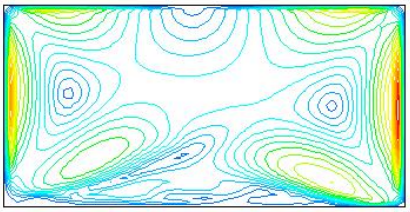

Figure 6.7: $Ra = 1.552 \times 10^{13}$

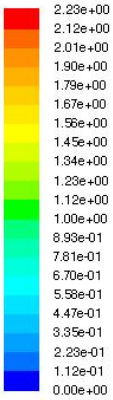

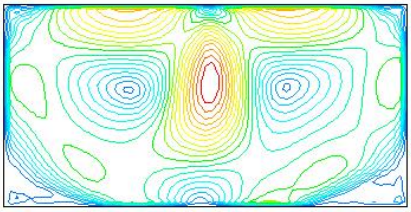

Figure 6.8: $Ra = 2.425 \times 10^{14}$

6.3 Contours of total temperature/Isotherms

The term "isotherm" refers to a line or curve on a temperature graph that joins two spots with the same temperature. Convection has a larger part in heat transfer as the Rayleigh number rises. It's clear that as the Rayleigh number rises, the maximum temperature falls. The highest temperature depicted is 290 degrees Kelvin in Figure 6.9, 288 degrees Kelvin in Figure 6.10, 282 degrees Kelvin in Figure 6.11, and 279 degrees Kelvin in Figure 6.12. The heat flow is portrayed as a series of contours that begin at the warm wall and terminate at the cool wall. It's also important to note that the buoyancy forces get stronger as the Rayleigh number goes up. This thins the thermal boundary layer along the hot wall and brings the hot spots closer to the centre. It is easy to see from the figures below how the Rayleigh number varies in relation to the overall temperature.

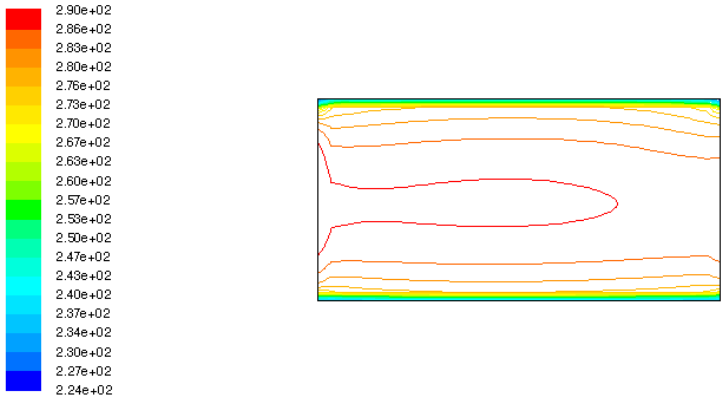

Figure 6.9: $Ra = 1.552 \times 10^{10}$

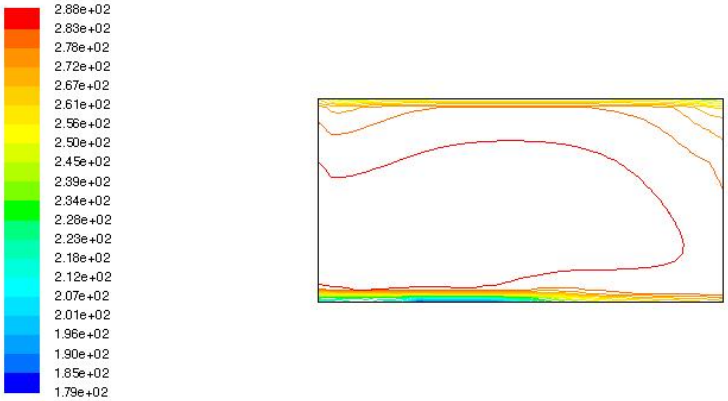

Figure 6.10: $Ra = 9.934 \times 10^{11}$

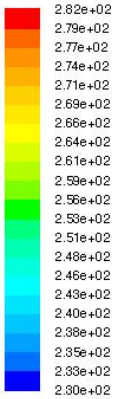

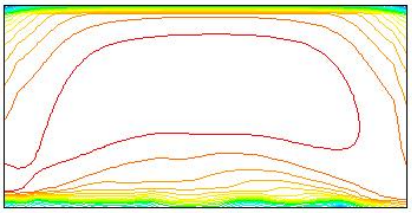

Figure 6.11: $Ra = 1.552 \times 10^{13}$

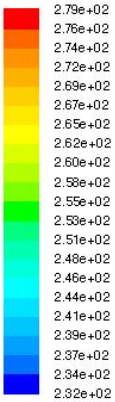

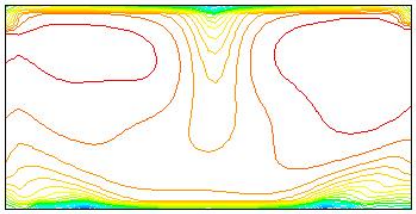

Figure 6.12: $Ra = 2.425 \times 10^{14}$

6.4 Contours of Turbulent Kinetic Energy

For this purpose, the results reveal that the kinetic energy of the turbulent fluid increases as the Rayleigh number increases. The following diagrams illustrate this point perfectly. The kinetic energy fluctuations, and hence the fluid velocity inside the enclosure, increase with increasing Rayleigh number. It is also discovered that at high-velocity regimes close to the heated wall, the Rayleigh number has a major impact on the flow structure of turbulent kinetic energy. The top wall has more kinetic energy than the lower wall.

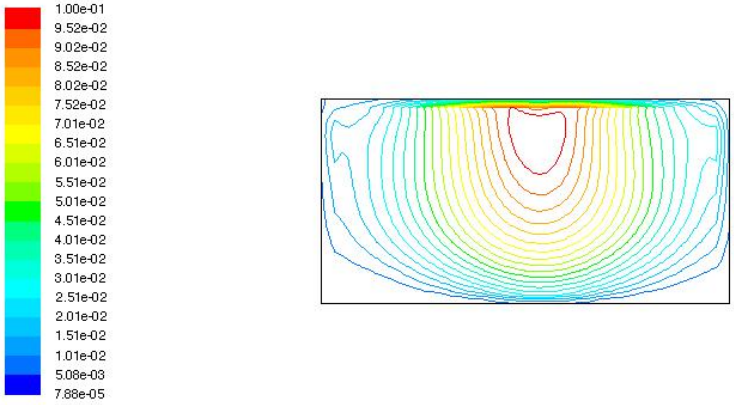

Figure 6.13: $Ra = 1.552 \times 10^{10}$

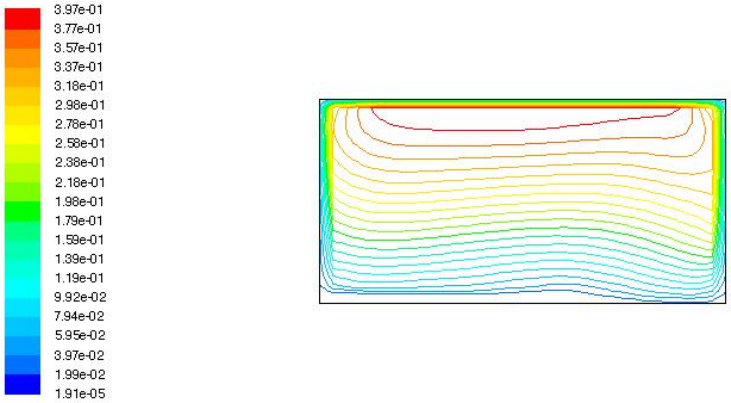

Figure 6.14: $Ra = 9.934 \times 10^{11}$

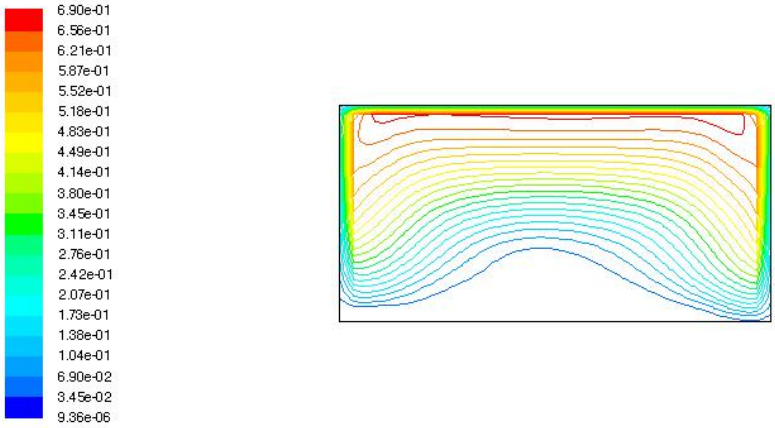

Figure 6.15: $Ra = 1.552 \times 10^{13}$

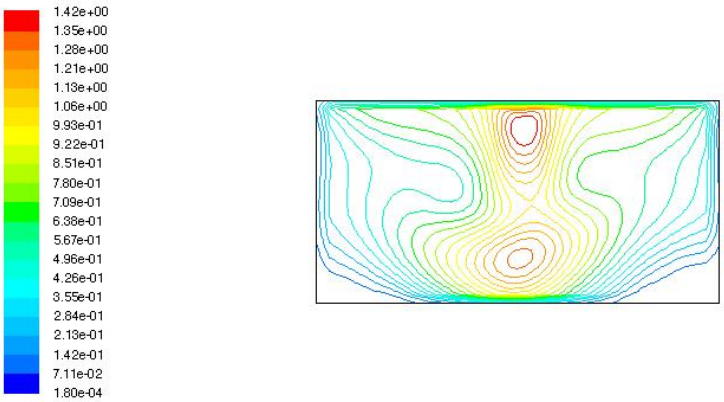

Figure 6.16: $Ra = 2.425 \times 10^{14}$

CHAPTER SEVEN

CONCLUSION AND RECOMMENDATIONS

7.1 Conclusion

The focus of this research was to use vorticity vector formulation to conduct a numerical simulation and investigation of natural turbulent flow inside a rectangular chamber filled with air. In order to accomplish this, we had established a number of specific objectives, all of which were met in the following ways:

In this work, we considered the partial differential forms of the Continuity Equation, the Navier-Stokes Equation, and the Energy Equation. These equations were statistically averaged and decomposed using the Reynolds Decomposition method. To complete the set of equations that defined turbulence, the resulting nonlinear equations comprising the Reynolds Stress equation were modeled by a k-ε turbulence model. Numeric data were set for k-ε turbulence model by application of vorticity stream function and vector potential formulation. The boussinesq estimation was used, which simplified the conservation equations. Three-point forward, central, and backward difference approximations discretized boundary-conditioned governing equations to numerically simulate the turbulent flow in the rectangular enclosure filled with air.

Streamlines, Velocity magnitudes, Isotherms and contours of kinetic energy were generated by FLUENT 6.2.3 for Rayleigh numbers $Ra = 1.552 \times 10^{10}$, $Ra = 9.934 \times 10^{11}$, $Ra = 1.552 \times 10^{13}$ and $Ra = 2.425 \times 10^{14}$ while keeping the aspect ratio of 2 constant. The results reveal that changing the Rayleigh number has an effect on fluid parameters including velocity and temperature. As a consequence of this, the magnitude of the velocity and the magnitude of the vortices both increase in tandem with an increase in the Rayleigh number. Maximum velocity was measured at 2.23 meters per second, and minimum velocity was measured at 0.308 meters per second.

For low Rayleigh numbers case, the temperature is higher than expected, and this is in relation to the way temperatures are distributed across the case. The flow becomes increasingly turbulent and chaotic

as the Rayleigh number grows, which leads to the temperature being distributed toward the center of the enclosure. At the lowest Rayleigh number, the temperature reached a maximum of 290 degrees Kelvin, while at the highest Rayleigh number, the temperature reached a maximum of 279 degrees.
A rise in the Rayleigh number is responsible for the accompanying rise in kinetic energy. The results show that as the Rayleigh number increases, the kinetic energy of the fluid in the domain's turbulent regions also increases. In addition, the higher the value of the Rayleigh number, the greater the kinetic energy fluctuations, and thus the greater the fluid velocity of the liquid within the container. At high-velocity regimes close to the heated wall, it has also been discovered that the Rayleigh number has a considerable influence on the flow structure as well as the turbulent kinetic energy.

7.2 Recommendation

The solution in natural convection and fluxes that are driven by buoyancy within a rectangular enclosure with a fixed aspect ratio and variable Rayleigh number was predicted numerically in this study. The enclosure's walls were adiabatic, with one being hot and the other opposite side being comparatively chilly. From this study it is recommended that further investigations be done in enclosures:-

(i) With the same measurements and temperature conditions using other models like $k-\omega$ SST model, RNG $K-\varepsilon$ model because in this case standard $K-\varepsilon$ model was used.

(ii) Changing the aspect ratio and enclosure size while maintaining the same Rayleigh number.

(iii) With a window installed at the top of the cold wall, as well as a comparing the results of this study with the distribution of streamlines and isotherms.

REFERENCES

Altaç, Z. and Uğurlubilek, N. (2016). Assessment of turbulence models in natural convection from two- and three-dimensional rectangular enclosures. *International Journal of Thermal Sciences*, 107:237–246.

Ampofo, F. and Karayiannis, T. (2003). Experimental benchmark data for turbulent natural convection in an air filled square cavity. *International Journal of Heat and Mass Transfer*, 46(19):3551–3572.

Awuor, K. O. and Gicheru, M. G. (2017). Numerical simulation of natural convection in rectangular enclosures.

Bansal, R. (2005). *A textbook of fluid mechanics*. Firewall Media.

Bernard, P. S. and Wallace, J. M. (2002). *Turbulent flow: analysis, measurement, and prediction*. John Wiley & Sons.

Chaabane, R., Kolsi, L., Jemni, A., Alshammari, N. K., and D'Orazio, A. (2021). Numerical study of the rayleigh–bénard convection in two-dimensional cavities heated by elliptical heat sources using the lattice boltzmann method. *Physics of Fluids*, 33(12):123605.

Currie, I. Fundamental mechanics of fluids, 1974. *&*, 41:40.

DOĞAN, M. and DOĞAN, D. (2017). Experimental investigation of natural convection heat transfer from fin arrays for different tip-to-base fin spacing ratios. *Isı Bilimi ve Tekniği Dergisi*, 37(1):147–157.

Doukkali, H., Abide, S., Lhassane Lahlaouti, M., and Khamlichi, A. (2018). Large eddy simulation of turbulent natural convection in an inclined tall cavity. *Numerical Heat Transfer, Part A: Applications*, 74(4):1175–1189.

Franke, R. and Rodi, W. (1993). Calculation of vortex shedding past a square cylinder with various turbulence models. In *Turbulent shear flows 8*, pages 189–204. Springer.

Itatani, K., Okada, T., Uejima, T., Tanaka, T., Ono, M., Miyaji, K., and Takenaka, K. (2013). Intraventricular flow velocity vector visualization based on the continuity equation and measurements of vorticity and wall shear stress. *Japanese Journal of Applied Physics*, 52(7S):07HF16.

Karanja, S., Sigey, J., Gatheri, F., and Kirima, E. (2017). Turbulent natural convection in an enclosure at varying aspect ratio.

Kubíček, M., Hlaváček, V., and Holodniok, M. (1976). Solution of nonlinear boundary value problems—x: The false transient method. *Chemical Engineering Science*, 31(8):727–731.

Kuznetsov, G. V. and Sheremet, M. A. (2010). Numerical simulation of turbulent natural convection in a rectangular enclosure having finite thickness walls. *International Journal of Heat and Mass Transfer*, 53(1-3):163–177.

Liu, J., Hussain, S., Wang, W., Xie, G., and Sundén, B. (2021). Experimental and numerical investigations of heat transfer and fluid flow in a rectangular channel with perforated ribs. *International Communications in Heat and Mass Transfer*, 121:105083.

Loksupapaiboon, K. and Suvanjumrat, C. (2021). Assessment of turbulence models for low turbulent natural convection heat transfer in rectangular enclosed cavity using openfoam. In *IOP Conference Series: Materials Science and Engineering*, volume 1137, page 012044. IOP Publishing.

Mayoyo, R., Sigey, J. K., Okelo, J. A., and Okwoyo, J. M. (2015). An investigation of buoyancy driven natural convection in a cylindrical enclosure.

Mugambi, F. M. (2021). *Numerical simulation of turbulent natural convection in a rectangular enclosure with localised heating and cooling*. PhD thesis, Kenyatta University.

Mutua, C. K. (2019). *A numerical Study Of Turbulent Natural Convection In A Rectangular Enclosure With Localised Heating and Cooling*. PhD thesis, Kenyatta University.

Ozoe, H., Yamamoto, K., Churchill, S., and Sayama, H. (1976). Three-dimensional, numerical analysis of laminar natural convection in a confined fluid heated from below.

Schiestel, R. (2010). *Modeling and simulation of turbulent flows*, volume 4. John Wiley & Sons.

Singh, A., Leonardi, E., and Thorpe, G. (1993). Three-dimensional natural convection in a confined fluid overlying a porous layer.

Sompong, P. and Witayangkurn, S. (2013). Natural convection in a trapezoidal enclosure with wavy top surface. *Journal of Applied Mathematics*, 2013.

Talukdar, D. and Tsubokura, M. (2021). Numerical study of natural-convection from horizontal cylinder at eccentric positions with change in aspect ratio of a cooled square enclosure. *Heat and Mass Transfer*, pages 1–23.

Tennekes, H., Lumley, J. L., Lumley, J. L., et al. (1972). *A first course in turbulence*. MIT press.

Versteeg, H. and Malalasekera, W. (1995). An introdution to computational fluid dynamics. *The finite volume method*.

Woods, L. C. (1954). A note on the numerical solution of fourth order differential equations. *Aeronautical Quarterly*, 5(4):176–184.